



# Hydrogeology and hydrogeochemistry of Nileschwaram river basin of Kerala, southern India

K.V. Sarath <sup>1,\*</sup>, Namitha Ajay<sup>1</sup>, Alka Absur<sup>2</sup>, V. Nandakumar<sup>2</sup>, E. Shaji <sup>1</sup>

<sup>1</sup>Department of Geology, University of Kerala, Kariavattom campus, Thiruvananthapuram, Kerala, 695581, India

<sup>2</sup>National Centre for Earth Science Studies, Ministry of Earth Sciences, Government of India, Akkulam, Thiruvananthapuram, Kerala, 695011, India

## ABSTRACT

A hydrogeochemical study was conducted in the Nileschwaram River Basin (NRB), Kerala, Southern India, to identify the mechanisms responsible for the chemical compositions of the groundwater and to document geo-hydrochemical behaviour with respect to drinking and agricultural supply standards. The groundwater samples were collected from bore wells, and dug wells to assess water quality variations. Residents of the basin face severe groundwater scarcity during the pre-monsoon season, impacting drinking water and domestic use. Over depends of bore wells, lacks of groundwater recharge, and the topographical features are contributed to drinking water shortages. The dominant hydrochemical facies of NRB is  $\text{Ca}^{2+}-\text{HCO}_3$  type. The concentrations of Fe and Mn, exceeding maximum permissible limits recommended by WHO. Detailed geochemical analysis, including petrography and X-Ray Fluorescence (XRF), revealed that these elements originate from the weathering of basement charnockite rocks and associated mafic and ultramafic rocks and subsequent rock-water interaction processes. This study aims to provide a multidimensional perspective to address this critical issue and ensure the implementation of appropriate strategies for sustainable water management to reduce water quality degradation of NRB.

## ARTICLE HISTORY

Received: 16 April 2025

Revised: 09 June 2025

Accepted: 11 June 2025

<https://doi.org/10.5281/zenodo.15642049>

## KEYWORDS

River basin  
Groundwater  
Rock-Water Interaction  
Groundwater quality  
Nileschwaram River Basin

## Highlights

- First time investigating the trace metal studies in groundwater of Nileschwaram river basin
- Petrography and XRF data are used for the characterization of trace metals in groundwater.
- The rock-water interaction process is the main reason for the enrichment of trace elements.

## 1. Introduction

The increasing global demand for water, driven by population growth, expanding irrigated agricul-

ture, and economic development, is straining water resources worldwide (Hanasaki et al., 2018; Wada et al., 2010; Hurtado et al., 2024). In regions with frequent water stress and extensive aquifer systems, groundwater is often tapped as an additional water source (Bhatnagar et al., 2024). However, excessive groundwater abstraction can lead to overexploitation and persistent depletion, causing groundwater levels to decline (Sophocleous, 2004; Gleeson et al., 2010; Taucare et al., 2024). This decline can have detrimental effects on natural streamflow, groundwater-fed wetlands, and related ecosystems.

Groundwater depletion, which is the reduction in the volume of groundwater in storage in the subsur-

\*Corresponding author. Email: [sarathgeo123@gmail.com](mailto:sarathgeo123@gmail.com) (KVS)

face, can lead to land subsidence, negative impacts on water supply, reduction in surface water flows and spring discharges, and loss of wetlands (Konikow and Kendy, 2005; Mays, 2013; Kuang et al., 2024; Munir et al., 2024). Groundwater depletion has been recognized as a global problem that threatens the sustainability of water supplies. Groundwater is being exploited extensively in many parts of the world with a massive increase in extraction in the past few decades due to the availability of new and cheaper drilling and pumping technologies (Barbier, 2019). Hydrogeologists refer to this drastic change in groundwater utilization as ‘the silent revolution,’ since it has occurred in many countries in an unplanned and totally uncontrolled manner (Stone et al., 2019).

The demand for good quality groundwater has increased with increasing population and developmental activities across the globe. Providing safe drinking water to the world’s 7.8 billion people is one of the greatest challenges of the century. At the beginning of 20<sup>th</sup> century, the groundwater quality issues were minimal and total dissolved solids and pH were the only parameters of concern (Shaji et al., 2021, 2024). However, during 21<sup>st</sup> century, there has been increased global attention on resolving groundwater quality issues. The chemical quality of groundwater varies significantly depending on the type of aquifers, duration of rock-water interaction and the inputs from various natural and nonnatural sources (Sarath et al., 2023).

During the last decade, groundwater contamination from various chemical constituents is being reported from aquifers throughout the world and often it becomes non-potable as the constituents exceed the limits prescribed by WHO. Geochemical processes during and after aquifer recharge can either improve or cause a deterioration of water quality (Maliva, 2020). In the recent years, pollution by arsenic (As) has become a serious issue of concern in view of its toxicity to humans (Polya et al., 2019). Arsenic contaminants in groundwater can also affect the health of the aquifers.

This study beheld into the sources of the trace elements that are present in phreatic groundwater and deeper aquifers, as well as the mechanisms that release them. There are not many studies on the process by which toxic elements from deeper aquifers are released into groundwater. In this scenario, where groundwater is the only source of drinking water in an area facing a water crisis before the Premonsoon

season, it is imperative to fully comprehend the concentrations of heavy metals and their sources. We have selected a watershed from southern India because it is crucial to understand these factors in order to safeguard the long-term management of this vital resource and to protect public health.

## 2. Study area

The study area located in Nileschwaram River Basin (NRB) of Kasaragod district, Kerala, southern India (Fig. 1a). The Nileschwaram river basin has a drainage area of 190 sq. km. and lies between north latitudes 12° 13’ and 12° 23’ and east longitudes 75° 05’ and 75° 17’. The river originates from Kinannur in Hosdurg Taluk at an elevation of 180 m above mean sea level. The Nileschwaram river joins the Kariangode river which in turn joins the Lakshadweep Sea. The river bed falls rapidly to 15 m above mean sea level within a short distance of 8 km (Fig. 1b). The entire basin area falls under the Kasargod district. The slope of the terrain varies significantly therefore, the rate of infiltration and the surface run off vary from place to place. The length of the river is 46 km in which the last 10 km experiences tidal effect (Fig. 1f).

### 2.1. Geology and Geomorphology

Geologically the area is dominated by high grade metamorphic granulite facies rock like charnockite and followed by patches of various gneissic rock units such as garnet gneiss, garnet biotite gneiss, granite gneiss and pyroxene granulites (Fig. 1c). Linear patches of high-grade rocks occur in the eastern and highland regions of NRB. Laterite is one of the major rock units in shallow to intermediate depth. Shallow coastal stretch is composed by younger clay and sand deposits (Fig. 1c). Among these, charnockite covers the major area.

Geomorphologically the NRB is divided into six category such as moderately dissected hills and valley, low dissected plateau, pediment pediplain complex, flood plain, coastal plain and water bodies. Major portion of the study area is covered by low dissected plateau followed by pediment pediplain complex. There is a no river mouth in the NRB (Fig. 1d). Physiographically the district can be divided into three district units viz. the coastal plains, the midlands, and the eastern highland regions. The coastal plains with an elevation of less than 10 m occur

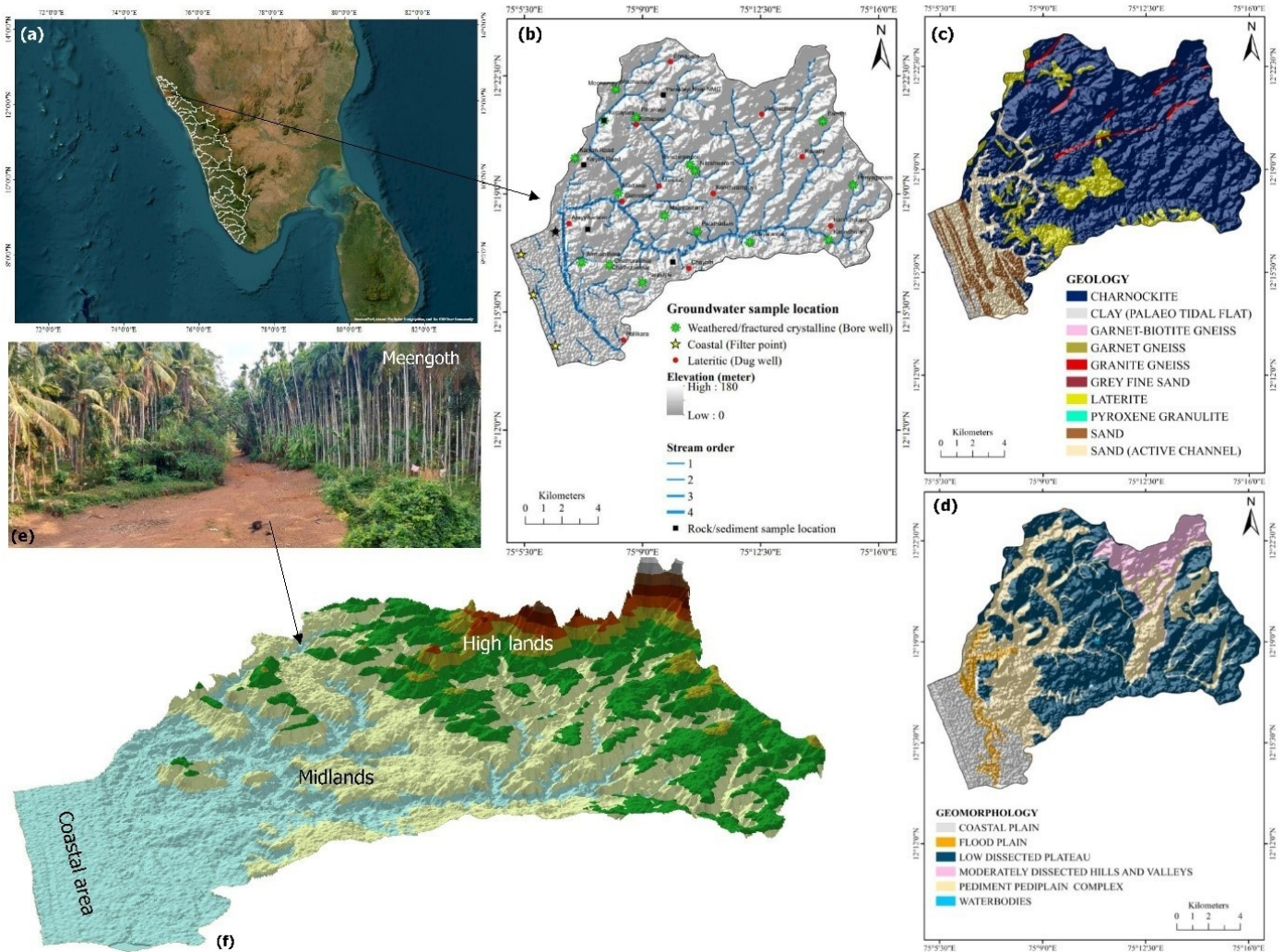


Fig. 1. (a). Location map of the study area, Nileschwaram River Basin (NRB) in Kerala, South India with groundwater sample locations overlying on the drainage map (b), (c) geology map. (d) geomorphology map (e) field photograph of 3<sup>rd</sup> order stream (f) 3D view of the NRB.

as a narrow belt of alluvial deposits parallel to the coast (Fig. 1d). The midland area is characterised by rugged topography formed by small hillocks separated by deep-cut valleys. The midland regions show a general slope towards the western coast. To its east is the highland region. The midland and hill ranges of the district present a rugged and rolling topography with hills and valleys. Along the midlands, the hills are mostly laterite and the valley is covered by valley-fill deposits (Fig. 1d&f).

## 2.2. Hydrogeology

The hydrogeological units mapped from the area include fractured crystallines tapped by bore wells (aquifer-1), laterites by dug well (aquifer-2), filter point wells in alluvium (aquifer-3) as shown in the Fig. 1b. Groundwater exists in unconfined conditions

within alluvium, laterites, and weathered crystalline mantle, whereas in deeper fractured crystallines it typically occurs under semi-confined to confined conditions. Laterite is the most widespread and extensively developed aquifer (Fig. 1b). The water level ranges from 4 m to 18.07 m bgl in pre-monsoon period and 1.5 to 15.5 m bgl in post monsoon period (Table 1).

The groundwater level above means sea level illustrated in the Fig. 2a. Duricrust, which tops the laterite, does not allow quick recharge from rainfall, resulting in a rapid decline in water levels (Fig. 2b). In well sections the laterite is usually followed by a thick layer of lithomarge clay, and the thickness range from 0.5 to 2.0 m (Fig. 2c&e). The weathered crystallines form the aquifer of limited potential, fractured crystallines are the important aquifer



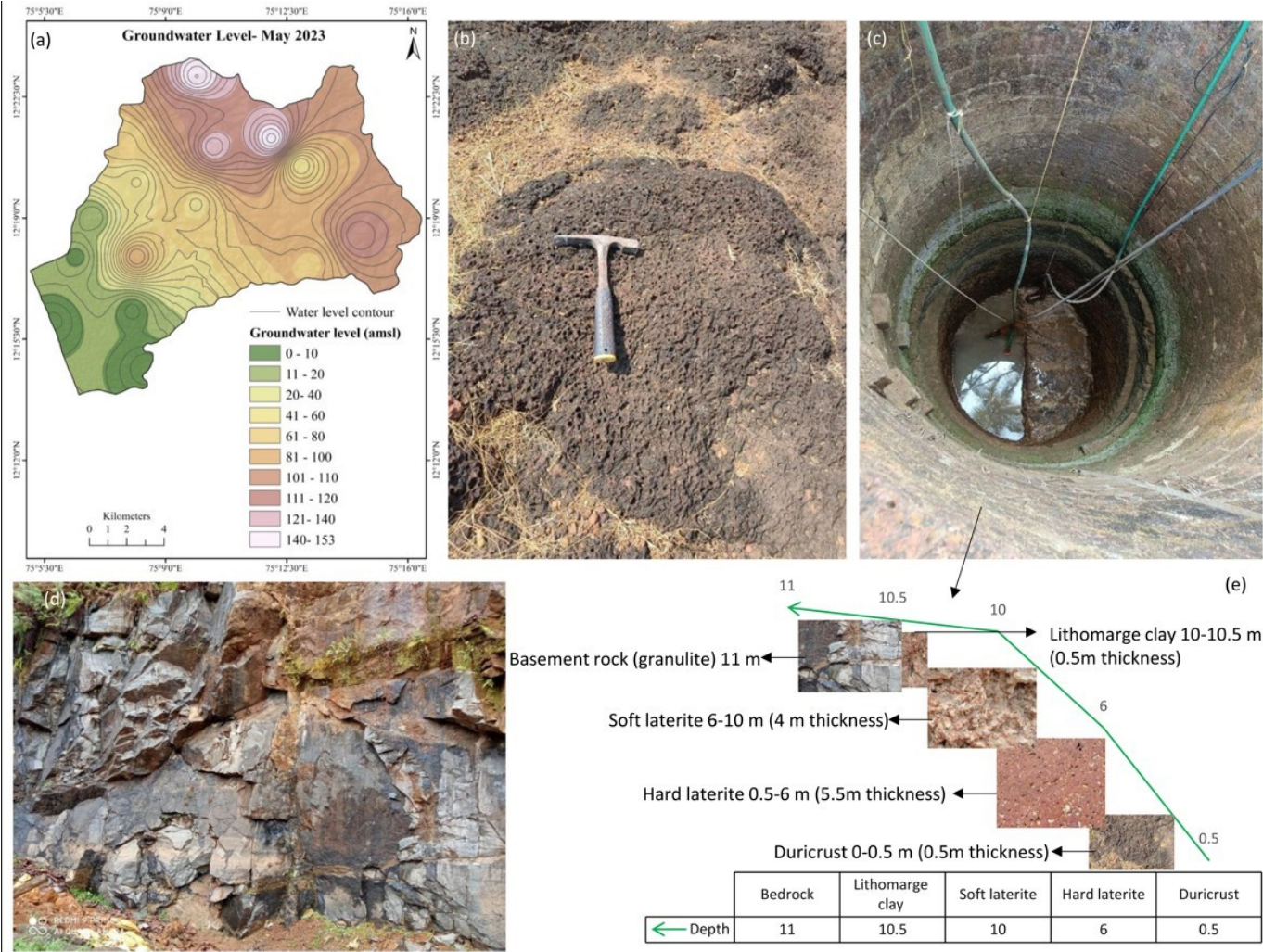


Fig. 2. (a) groundwater level above mean sea level (b) thick duricrust layer (c) dug well shows fractured basement rocks at a depth of 11 m (d) fractured charnockites (e) lithographic model of a well near to coastal area.

at depth of >50 m. Fig. 2d shows the fractured crystalline charnockites with leakage of groundwater. In the fractured crystalline aquifer ground water occurs under semi-confined to confined conditions.

2.3. Groundwater scenario

The area receives an average annual rainfall of 4000 mm. The south-west monsoon (June–August) accounts for 65% of annual precipitation, while the north-east monsoon (September–November) accounts for 25% and the pre-monsoon showers account for 10% of annual rainfall. Despite the fact that the annual average rainfall is high, the majority of it is concentrated in only 3–4 months of the year, leaving the remainder of the year particularly dry.

According to studies by the Central Ground Water Board (CGWB). The study area experiences severe drought during summer, leading to acute water

scarcity in the hilly areas due to the drying up of dug wells (Fig. 3a) Another concern is the overdependence on borewells for extracting water from deeper aquifers. From the local survey conducted around the study area from the dug well inventory data (Table 1) shows that rapid declining of water table. This is happened due to high porous and permeable nature of laterite and vertical movement of groundwater, also influence the over dependence of bore well pumping and increasing number of borewells and population density.

From the field observation, it can be inferred that the groundwater is declining at an alarming rate. Wells, of 2<sup>nd</sup> and 3<sup>rd</sup> order streams from the area has dried up. This situation is given in the Fig. 3 which shows the representation of the groundwater decline baseflow of the stream has reduced significantly, the stream shows influent nature. The Fig. 3a&b repre-



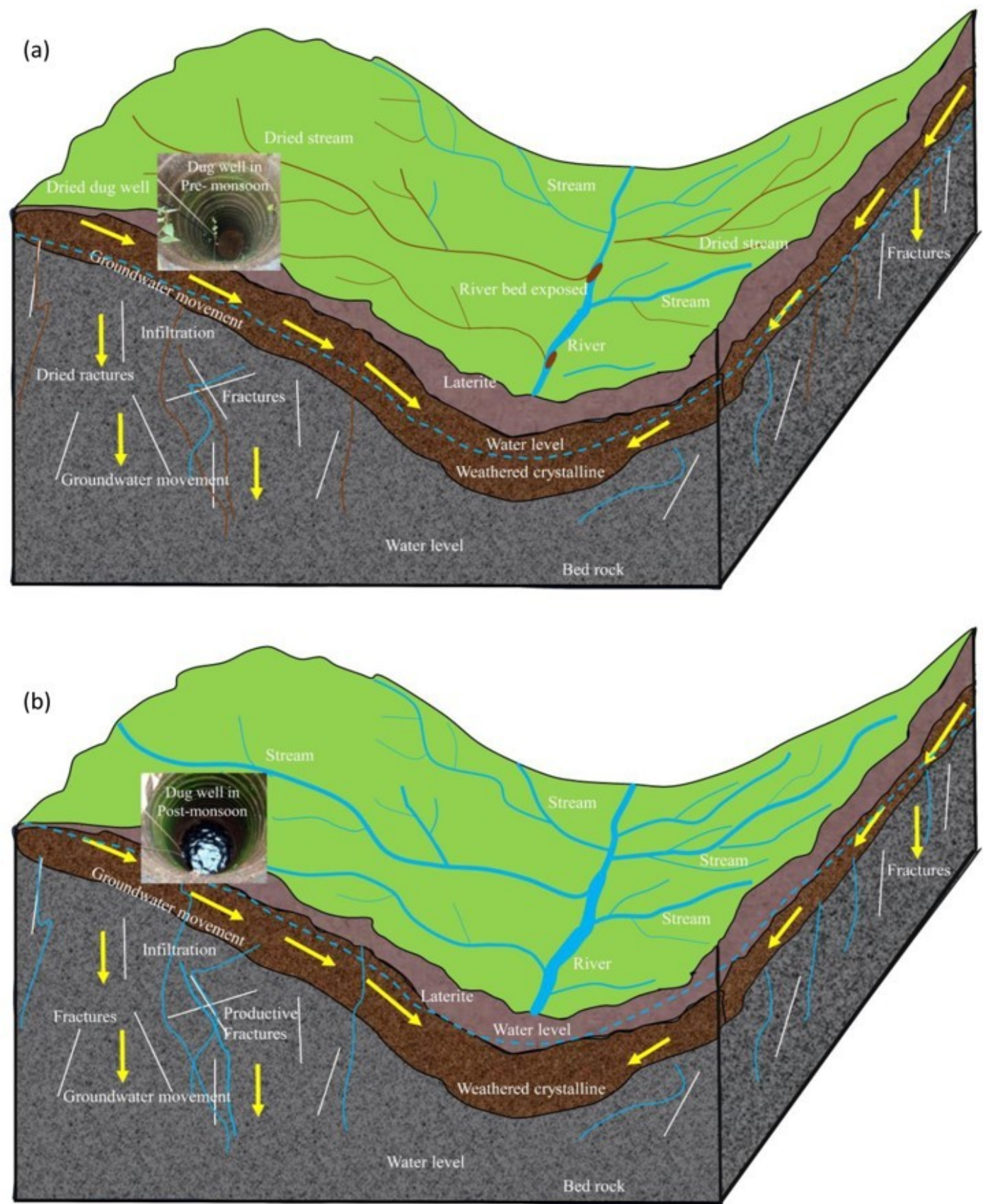


Fig. 3. (a) Pre-monsoon and (b) post monsoon surface-groundwater condition of NRB. Most of the dug wells and stream channel facing water shortage and drying. Post monsoon season water is saturated with stream channel and vadose zone. The figure is made up based on the field investigations.

Table 1. Groundwater level monitoring data.

Sl No	Location	Latitude	Longitude	Elevation(m)	MP(m)	Water Level Pre-monsoon	Water Level Post-monsoon
1	Arayyikadavu	12.317	75.115	48	0	2	4
2	Guruvanam	12.298	75.136	103	0.7	3	3.7
3	Mundott	12.351	75.173	140	0.8	4.2	5.25
4	Kanchirampoil	12.323	75.164	89	0.85	9.5	14.9
5	Chathurakinari	12.272	75.134	45	0.65	8	11.3
6	Paraklayi	12.365	75.16	129	0.82	10.5	14.8
7	Kottapara	12.353	75.131	93	0.85	7.8	10.9
8	Kollampara	12.295	75.22	106	0.8	15.5	18.07
9	Pallikara	12.244	75.14	34	0.89	4.3	6.52
10	Karindhalam	12.308	75.243	136	0.6	8.7	13
11	Ennapara	12.385	75.165	164	0.75	9.4	12.6
12	Vengacherry	12.355	75.201	156	1	4.5	7.35
13	Kalyan Road	12.334	75.136	75	0.85	5.2	8.5
14	Kuvatty	12.342	75.215	78	1	4.3	7
15	Puthiyavalap	12.298	75.107	41	0.75	2.4	3.75
16	Ozhinjalap	12.267	75.096	33	0.7	1.5	2.95

sents an image made by the combination of the field photographs from the pre- and post-monsoon season. It is observed that during pre-monsoon season, the streams have become dry and the bed have been exposed (Fig. 1e). Normally stream bed is the ground surface of water level, but from the present conditions it can be inferred that the baseflow has gone below the stream bed. From the local survey, it is found that the present condition has been ongoing for some years now. This has led to the drying of wells in high elevation areas as well areas near the stream bed. This decline in water level can be attributed to low precipitation levels. The Fig. 3b illustrates secondary fracture zones which have become dry, this caused the borewells and dug wells in the area to dry up. In the post monsoon season well are recharged with precipitation and groundwater infiltration. Rainfall recharges the river basin, but steep slope nature of the terrain causes rapid surface runoff the stream and high velocity causes drying up the river within the few months.

### 3. Materials and methods

#### 3.1. Groundwater sampling

Detailed hydrogeological studies were conducted in and around the Nileshwaram river basin for ten days from 9 to 19 May 2023. The length and breadth of the study region were covered by taking different travers and established thirty-eight observation sites. The details of 38 observation wells. 14 dug wells, 18 bore wells, and 6 filter point well samples were monitored for sample collection. Groundwater samples were collected at regular interval covering 190 km<sup>2</sup>. Twenty-nine locations of nearby river basin were additionally visited for hydrogeological understanding.

Sections of wells were seen and noted. The observation wells' diameter, total depth, and depth to the water level were measured, sampling locations are given in Fig. 1a. Samples were collected in polyethylene bottles and bottles were rinsed 3–5 times with the same water samples before filling. Analysis of groundwater quality data are presented in the Table 2.

#### 3.2. Hydrochemical analysis

Water quality parameters like pH, Electrical Conductivity (EC), and Total Dissolved Solids (TDS) were measured in the field. The samples were analysed in the chemical laboratory of the Department of Geology, University of Kerala. Analysis was carried out as per the standard methods suggested by APHA (2012). Major ions like Ca<sup>2+</sup>, Na<sup>+</sup>, K<sup>+</sup>, Mg<sup>2+</sup> and NO<sub>3</sub><sup>-</sup> were analysed, alkalinity was measured by titration, Ca<sup>2+</sup>, Total Hardness (TH), and Mg<sup>2+</sup> analysed using titration with EDTA. Cl<sup>-</sup> concentration was determined by using Argentometric titration. UV visible spectrophotometer was used for analysis of sulphate (Turbidimetric method), phosphate (Ascorbic acid method), and NO<sub>3</sub><sup>-</sup>. Na<sup>+</sup> and K<sup>+</sup> were analysed using a flame photometer. The analytical precision of the measurements of cations and anions is indicated by the ionic balance error, which has been computed based on ions expressed in milliequivalent per litre (mEq/l). The values were observed to be within the standard limit of  $\pm 3\%$ .

Trace elements, heavy metals and PGEs were analysed by using Q-ICP MS at Inter-University Accelerator Centre (IUAC), at the Geochronology lab New Delhi, India. Q-ICP MS is a low-resolution, versatile, and rapidly growing multi-element trace/ultra-trace element analysis mass spectrometer that can

Table 2. Groundwater quality analysis of major ions.

SL No	Location	pH	EC	TDS	TA	TH	Ca	Mg	Na	K	CO <sub>3</sub>	HCO <sub>3</sub>	Cl	SO <sub>4</sub>	PO <sub>4</sub>	NO <sub>3</sub>
1	Arayyikadavu	5.49	195	97.64	96	42	13.62	1.944	53.5	4.03	0	117	142.1	0.43	4.45	0.14
2	Guruvanam	6.15	25.3	12.66	52	16	5.61	0.486	6.74	0.58	0	63.4	68.07	0.44	0.68	0.44
3	Mundott	5.95	68.4	34.24	64	16	6.41	0.486	17.4	3.23	0	78.0	68.07	2.86	0.72	0.04
4	Kanchirampoil	6.62	138	69.29	72	52	24.84	0.486	26.4	4.62	0	87.8	66.07	0.52	2.62	0.01
5	Kanchirampoil	5.79	42.5	21.31	64	18	3.206	2.431	8.27	1.29	0	78.0	54.05	0.5	0.5	0.01
6	Madikkai	6.46	163	81.74	260	56	21.643	0.486	25.8	4.71	0	317	72.07	0.57	2.11	0.02
7	Chathurakinar	8.07	564	282.4	960	18	6.412	0.486	406	14.5	96	976	60.06	186	1.93	0.32
8	Chathurakinar	6.12	50.2	25.13	52	12	6.412	0.486	12.3	2.25	0	63.4	62.06	2.66	0.43	0.16
9	Paraklayi	7.02	170	85.54	344	96	24.849	8.265	17.3	1.94	14.4	390	56.06	0.75	2.53	0.01
10	Paraklayi	6.52	99.8	49.93	192	38	14.428	0.486	18.8	2.46	0	234	40.04	0.72	2.15	0.03
11	Kottapara	7.91	206.	100.8	248	68	21.643	3.403	14.4	4.44	9.6	283	56.06	3.09	2.16	0.04
12	Kottapara	6.12	41.8	20.93	52	20	6.412	0.972	8.66	1.52	0	63.4	48.05	0.45	0.98	0.0
13	Moonamayil	6.9	126	63.21	220	44	16.833	0.486	21.6	3.64	14.4	239	56.06	1.28	2.98	1.01
14	Periyaganam	6.7	153	110	248	66	24.849	0.972	13.6	2.57	0	302	40.04	16.9	2.42	0.18
15	Kollampara	5.4	26.8	26.2	256	86	30.460	2.431	14.5	3.44	48	214.	46.05	55.5	3.03	0.19
16	Kollampara	7.05	211	149	188	14	4.008	0.972	7.59	0.73	0	229	44.04	1.42	0.74	0.98
17	Chayoth	7.3	193	138	28	86	32.865	0.972	13.2	3.63	0	34.1	40.04	76.4	2.52	0.75
18	Puthiyavalap	6.86	237	168	228	50	29.659	0.486	19.2	7.95	0	278	58.06	18.0	1.57	3.61
19	Puthiyavalap	6.76	58	41.6	64	16	7.2144	0.972	11.8	0.48	0	78.0	54.05	1.00	0.69	0.16
20	Ozhinjalap	8.07	156	117	208	70	27.254	0.486	10.9	2.59	0	253	52.05	8.02	1.35	0.58
21	Ozhinjalap	6.45	206	146	232	60	22.444	0.972	22.3	9.48	0	283.	78.08	49.1	1.18	0.80
22	Pallikara	5.68	79.7	56.9	52	30	9.6192	1.458	11.8	2.43	0	63.4	44.04	4.94	1.13	2.64
23	Thaikadapuram	6.4	120	85.5	124	50	15.230	2.917	11.7	5.32	0	151	54.05	5.15	1.10	0.68
24	Kanhangad	7.08	948	258.7	700	252	102.60	2.917	48.9	10.37	91.2	668	78.08	128.	0.69	0.70
25	Mayalagad	8	131	68	107.3	100	25.648	4.213	24.3	3.6	0	107	23.98	5.38	1.04	0.15
26	Karindhalam	7.7	195	94.42	146.4	172	33.663	10.30	23.2	2.9	0	146	21.9	48.0	0.96	0.33
27	Ambalathara	6.17	64.9	43.82	214.7	56	14.427	2.341	12.7	4.5	0	214	21.98	4.30	0.75	0.17
28	Banam	6.86	220	113.6	136.6	200	41.678	11.23	15.2	3.2	0	136	21.98	8.91	0.95	0.35
29	Paraklyai	6.9	138	71.41	107.3	92	24.045	3.745	21	4.9	0	107	15.99	6.39	0.97	0.20
30	Palathadam	6.1	26	11.15	24.4	24	4.809	1.404	4.7	0.49	0	24.4	21.98	2.65	0.38	0.16
31	Kalyan Road	6.7	306	155	161.0	184	70.532	0.936	33.8	4	0	161.	31.98	8.5	0.81	1.36
32	Nileshwaram	7.1	97	64.87	87.84	84	35.266	0.468	3.6	0.8	0	87.8	29.98	9.97	0.73	0.71
33	Malppachery	7.4	256	132.4	122	184	44.884	8.427	18.2	3.5	0	122	35.98	14.9	1.23	0.29
34	Karindhalam	7.8	90.6	46.8	48.8	80	27.251	1.404	9.94	2.9	0	48.8	17.99	4.22	0.61	0.70
35	Ennapara	5.87	28.5	14.76	24.4	20	6.412	0.468	5.8	0.75	0	24.4	17.99	8.32	0.69	1.45
36	Vengacherry	5.45	25.0	12.93	43.92	20	4.809	0.936	6.2	0.33	0	43.9	17.99	2.99	0.43	0.45
37	Kalyan Road	5.6	44	22.3	39.04	20	4.809	0.936	8.7	1.4	0	39.0	27.98	4.52	0.55	2.07
38	Kuvatty	5.1	72	39.6	29.28	132	9.618	12.64	11.4	5.6	0	29.2	33.98	9.79	0.46	0.22

analyse a wide range of liquid samples and matrices. A compact high-performance Q-ICP MS (Model: iCAPQ, Thermo Fisher Scientific) has produced bulk trace element data regularly. Milli-Q deionized water containing 1% HNO<sub>3</sub> acid was analysed to monitor background intensities and Background equivalent concentration (in ppb). For the quality control and quality check standard multi-element solution (25 ppb from VHG Labs and 5 ppb PGEs reference standard) was measured at intervals of every ten samples as unknown. Commercial multi-element standard solution from VHG Labs was used as standards to perform the calibration (1–100 ppb). For PGEs, a multi-element standard solution from Inorganic ventures was used. For data validation, a standard multi-element solution (VHG Labs and inorganic ventures) of known concentration was run considering an unknown sample with an interval of 10 samples and the % offset observed was less than 10%. The precision of measurements is better than 5% RSD for all elements. All results are an average

of three replicate analyses per measurement.

The thematic maps are prepared using ArcGIS. Statistical analysis of the hydrochemical data was performed using Microsoft Excel software.

### 3.3. Rock analysis

Rock and mineral samples were collected from Kanthampara area such rocks are charnockites, mafic and ultra mafic include rare lode stone. Ten polished thin sections were prepared for petrographic study including two samples for ore microscopic study by using Buhler USA and Struers-Labpol facilities available at National Centre for Earth Science Studies (NCESS), located in Thiruvananthapuram, India. Ultramafics from Kanthampara is selected for major element oxides using CAMECA SXFive-Tactis Electron Probe Microanalyzer (EPMA) equipped with five wavelength dispersive spectrometers. The operating conditions are: 15 kV accelerating voltage, 20 nA beam current, and 1 mm beam diameter. The elements and X-ray lines used for silicate mineral anal-



ysis include Fe, Si, Al, K, Na, P, Ti, Mg, Mn, and Ca. All of the elements were quantified using a peak counting time of 10 s and a background time of 5 s. Quantification methods were used for all elements. Background intensities were measured on both sides of the peak during half of the peak time. Data reduction was done using the X-Phi method.

Representative ten samples from NRB were collected for whole rock geochemical analyses. For the geochemical analysis the samples were crushed into small chips with a jaw crusher and finely powdered with a chrome-steel ring mill at the thin section and sample preparation was carried out at the laboratory of NCESS. Major elements in pressed powder pellets (boric acid binder) were analysed using Bruker Pioneer S8 Tiger WD-XRF at NCESS. The S8 Tiger features a goniometer with seven crystals (LiF 200, LiF 220, PET, XS-55, XS-N, XS-C, and XS-B), a 75-sample automatic loading system, a 4 kW Rh X-ray tube, and 0.23°, 0.46°, 1°, and 2° collimators. GPS, JG-1, and G2 were utilised as calibration standards. The data was reduced using the SPECTRAplus software.

## 4. Results

### 4.1. Hydrogeochemistry

Piper is a trilinear diagram made up of anion and cation equilateral triangles that are connected by a common baseline. The diamond plot formed by these anion and cation triangles is used to classify different types of water. The percentages of each cation and anion are plotted, and the concentrations are expressed in milliequivalents per litre. The diamond plot intertwines the relative proportions of cation-anion combinations of specific water samples, resulting in specific water types based on the prominent hydrochemical facies. The piper divides water into four basic types based on its location near the four corners of the diamond plot. Water with a plot in the top corner of the diamond has a high  $\text{Ca}^{2+} + \text{Mg}^{2+}$  concentration as well as a high  $\text{Cl}^- + \text{SO}_4^{2-}$  concentration. The water plots in the upper left corner are high in  $\text{Ca}^{2+}$ ,  $\text{Mg}^{2+}$ , and  $\text{HCO}_3^-$  and thus have a temporary hardness character. The bottom corner of the plot represents alkali carbonate water type ( $\text{Na}^+ + \text{K}^+$  and  $\text{HCO}_3^- + \text{CO}_3^{2-}$ ), while the plot near the right corner represents saline water type ( $\text{Na}^+ + \text{K}^+$  and  $\text{Cl}^- + \text{SO}_4^{2-}$ ).

Fig. 4a illustrates the Hill Piper Diagram of the study area, from the piper diagram, the predominant hydrogeochemical facies of samples was  $\text{Ca}^{2+}\text{--Mg}^{2+}\text{--HCO}_3^-$  with Temporary Hardness water type in all the groundwater samples collected from the study area except two samples from bore wells of Banam and Malpacherry fall under the mixed type category. The dug well samples belong to the dominance  $\text{Na} > \text{Ca} > \text{Mg} > \text{K}$  cations and  $\text{HCO}_3^- > \text{Cl}^- > \text{SO}_4^{2-} > \text{CO}_3^{2-}$  anions. The bore well samples belong to the dominance  $\text{Ca} > \text{Na} > \text{Mg} > \text{K}$  cations and  $\text{HCO}_3^- > \text{Cl}^- > \text{SO}_4^{2-} > \text{CO}_3^{2-}$  anions. Filter point well samples belong to the dominance  $\text{Na} > \text{Ca} > \text{Mg} > \text{K}$  cations and  $\text{Cl}^- > \text{HCO}_3^- > \text{SO}_4^{2-} > \text{CO}_3^{2-}$ . The alkaline earth metals (Ca, Mg, Sr, and Ba) slightly predominate over alkali metals (Na, K, and Li) in the groundwater. Weak acids ( $\text{HCO}_3^-$ ) exceed strong acids ( $\text{Cl}^-$  and  $\text{SO}_4^{2-}$ ).

The hydrogeochemistry of hard crystalline terrains is inherently complex. Crystalline environments have distinct geological and hydrogeological properties. Unlike sedimentary aquifers, which have well-developed porosity and relatively homogeneous flow paths, hard rock aquifers rely on secondary porosity (fractures, joints, and faults) to move groundwater. These features differ greatly in depth, connectivity, and aperture, resulting in irregular flow paths, localized water-rock interactions, and highly variable residence times (Chandra, 2015). Geochemical processes in these terrains are largely driven by the slow weathering of silicate minerals such as feldspar, biotite, and hornblende, which release a range of ions ( $\text{Na}^+$ ,  $\text{Ca}^{2+}$ ,  $\text{Mg}^{2+}$ ,  $\text{K}^+$ ,  $\text{HCO}_3^-$ ) and minimal thickness of soil profile and lack of residence time for rock water interaction process control the hydrogeochemical facies and mainly evolving water types, from  $\text{Ca}\text{--HCO}_3$  or mixed types.

Furthermore, cation exchange processes and the mixing of young and old groundwater trapped in fractures distort expected ion ratios, contributing to ionic balance errors even when lab analyses are precise. Because hard rock aquifers are naturally heterogeneous, even closely spaced sampling locations can produce significantly different chemical compositions, reinforcing the illusion of analytical error. While fewer comprehensive hydrogeochemical studies have historically been conducted in crystalline terrains, the observed data variability is a true reflection of natural processes rather than methodological flaws.

All major ions were within India's desirable limits for water Quality (Bureau of Indian Standards)



Table 3. Groundwater quality analysis of trace metal.

Label	Location	Li	Al	V	Cr	Mn	Fe	Co	Ni	Cu	Zn	As	Sr	Pd	Ag	Cd	Ba	Pb
Sample-1	Ajanur Beach	0.36	4.36	0.59	0.53	383.44	6.88	0.43	2.06	2.78	7.48	0.21	120.61	0.037	0.063	0.068	209.511	0.247
Sample-2	North Ajanur	0.86	5.18	2.85	0.71	9.97	5.32	0.37	2.37	2.34	21.42	3.14	125.30	0.031	0.082	0.102	94.433	0.457
Sample-3	North Ajanur	5.13	2.37	0.83	0.47	1337.17	11.32	0.63	0.87	1.20	2.82	0.92	1036.93	0.097	0.566	0.023	41.334	0.013
Sample-4	Kottapara	0.46	2.58	0.67	0.39	5.08	4.61	0.31	0.64	0.44	7.49	0.07	50.37	0.013	0.001	0.020	41.829	0.014
Sample-5	Kottapara	0.06	23.33	0.59	0.55	30.80	44.26	0.49	1.25	2.49	7.13	0.13	22.25	0.004	0.021	0.062	47.745	0.488
Sample-6	Parakkalayi	0.34	9.64	0.56	0.53	50.16	60.70	0.54	1.26	2.60	4.49	0.05	55.44	0.003	0.029	0.062	73.114	0.359
Sample-7	Parakkalayi	0.26	20.04	0.57	0.63	128.99	101.57	0.96	1.79	2.99	21.73	0.08	38.25	0.000	0.108	0.066	104.424	0.695
Sample-8	Moonamayil	0.60	13.64	0.56	0.43	5.82	372.67	0.36	1.31	2.73	7.63	0.07	60.52	0.003	0.033	0.068	58.962	0.469
Sample-9	Meengoth	0.16	32.46	0.56	0.45	18.01	67.31	0.82	16.11	5.03	9.28	0.08	35.54	0.004	0.000	0.062	103.342	0.582
Sample-10	Kanthampara	0.56	1.68	0.55	30.00	4.51	13.99	0.33	0.74	0.70	2.71	0.05	47.92	0.024	0.124	0.019	58.164	0.020
Sample-11	Kanthampara	0.58	5.63	0.57	45.60	19.60	34.33	0.34	1.25	2.92	4.23	0.08	48.14	0.002	0.002	0.016	46.101	0.187
Sample-12	Arayyikadavu	0.00	8.95	0.55	0.32	4.44	12.31	0.33	0.43	0.33	0.31	0.02	1.37	0.030	0.000	0.003	1.987	0.068
Sample-13	Guruvanam	0.00	3.98	0.53	0.31	0.64	0.11	0.31	0.45	0.34	0.30	0.00	0.21	0.000	0.000	0.000	1.605	0.014
Sample-14	Mundott	0.00	4.21	0.54	0.31	2.16	2.62	0.31	0.41	0.27	0.19	0.03	0.41	0.000	0.000	0.005	1.923	0.032
Sample-15	Kanchirampoil	0.10	3.37	0.53	0.30	0.74	2.25	0.30	0.44	0.26	0.25	0.00	3.79	0.000	0.000	0.002	7.876	0.027
Sample-16	Kanchirampoil	0.00	4.13	0.54	0.31	1.25	1.24	0.31	0.46	0.24	0.30	0.00	0.35	0.000	0.000	0.003	2.234	0.047
Sample-17	Madikkai	0.04	3.01	0.53	0.30	3.07	3.88	0.35	0.53	0.21	0.15	0.00	3.54	0.000	0.000	0.001	3.183	0.015
Sample-18	Chathurakinar	0.06	2.96	0.54	0.30	0.43	0.13	0.30	0.39	0.18	0.02	0.01	0.54	0.000	0.000	0.000	0.699	0.0
Sample-19	Chathurakinar	0.06	3.19	0.53	0.30	0.96	4.17	0.32	0.47	0.23	0.16	0.02	0.45	0.000	0.000	0.001	1.578	0.012
Sample-20	Manikoth	0.00	2.35	0.54	0.30	0.53	0.77	0.30	0.47	0.34	0.34	0.00	3.50	0.000	0.000	0.002	1.837	0.017
Sample-21	Chettukundu	0.00	2.91	0.54	0.30	1.04	0.30	0.32	0.49	0.27	0.22	0.01	0.79	0.000	0.000	0.003	2.473	0.014
Sample-22	Chettukundu	0.00	2.88	0.54	0.30	1.12	7.71	0.31	0.47	0.28	0.18	0.01	0.75	0.000	0.000	0.000	2.625	0.051
Sample-23	Kanhangad	0.02	2.37	0.57	0.30	0.47	1.08	0.30	0.48	0.27	0.18	0.02	12.33	0.007	BDL	0.007	1.685	0.001

Table 4. Descriptive statistics for the analyzed physicochemical parameters of NRB and comparison with national standard water quality requirements for drinking purposes.

Parameters	Cations					Anions		TDS	pH	TH	EC
	K <sup>+</sup>	Na <sup>+</sup>	Ca <sup>+</sup>	Mg <sup>2+</sup>	Cl <sup>-</sup>	SO <sub>4</sub> <sup>2-</sup>	HCO <sub>3</sub> <sup>-</sup>				
Unit	mg/L	mg/L	mg/L	mg/L	mg/L	mg/L	mg/L	mg/L		mg/L	S/cm
Max	14.5	406.5	102.6	12.64	142.15	186.7	976	282.4	8.07	252	948.5
Min	0.33	3.6	3.2	0.46	15.99	0.43	24.4	11.15	5.1	12	25.02
Mean	3.60	26.91	21.74	2.52	46.82	18.87	180.04	82.44	6.62	69.57	157.34
National Standard (Max)	Not available	200	200	100	1000	400	600	2000	6.5-8.5	450	2250

Table 5. Descriptive statistics for the analyzed trace metals in NRB and comparison with Bureau of Indian Standards (BIS) and World Health Organization (WHO) for water quality requirements for drinking purposes. Few trace metals such as Li, V, Co, Sr, Pd, and Ag does not have a guideline value for drinking water purpose.

Parameters	Li	Al	V	Cr	Mn	Fe	Co	Ni	Cu	Zn	As	Sr	Pd	Ag	Cd	Ba	Pb
Unit	g/L	g/L	g/L	g/L	g/L	g/L	g/L	g/L	g/L	g/L	g/L	g/L	g/L	g/L	g/L	g/L	g/L
Max	5.13	32.46	2.85	45.6	1337	2952	0.96	16.11	5.03	21.73	3.14	1036	0.09	0.5	0.10	209	0.69
Min	0	1.68	0.53	0.3	0.43	0.11	0.3	0.39	0.18	0.02	0	0.21	0	0.001	0	0.69	0
Mean	0.41	7.18	0.66	3.64	87.40	33.0	0.40	1.52	1.28	4.30	0.21	72.5	0.01	0.04	0.02	39.5	0.16
National Standard	-	30	-	50	30	1000	-	20	1500	5000	10	-	-	-	3	700	10
WHO Standard	-	200	-	50	300	300	-	20	2000	3000	10	-	-	-	3	700	10

and the desirable permissible limits of the WHO (Table 4). The concentration of TDS varied from 11.15 to 282.4 mg/L indicating fresh water. Generally, the groundwater in the up-gradient samples contained mostly HCO<sub>3</sub><sup>-</sup> and Ca<sup>2+</sup>, and the concentrations of Na<sup>+</sup>, SO<sub>4</sub><sup>2-</sup>, and Cl<sup>-</sup> increase down-gradient due to mineral dissolution along groundwater flow paths and near to coastal area. Slightly hard water is not well distributed across most of the study area, while hard water is mainly observed in the areas near shore lines. Soft water can be observed in entire the study area, which is due to recharge from rainwater with low concentrations of Ca and Mg.

1:1 ratio plot of (Fig. 4c-f) HCO<sub>3</sub><sup>-</sup> vs Na<sup>+</sup>, HCO<sub>3</sub><sup>-</sup> vs Ca<sup>2+</sup>, HCO<sub>3</sub><sup>-</sup> vs Mg<sup>2+</sup>, HCO<sub>3</sub><sup>-</sup> vs K<sup>+</sup> respectively. The 1:1 ratio plot suggest that HCO<sub>3</sub><sup>-</sup> and Ca<sup>2+</sup> are the dominant anion and cation in groundwater which is derived from weathering of plagioclase feldspar (anorthite and albite) and K and Na

is sourced from dissolution alkali feldspar (orthoclase and microcline). Little amount of Ca and Mg is derived from weathering of ferromagnesium minerals (pyroxene and biotite) and there is a no sources minerals for excess Ca, Mg ions in groundwater like magnesite, carbonates and evaporates. Field evidence support silicate weathering, ruled out the dissolution of halides and calcite.

4.2. Trace metals in groundwater

The Q-ICP MS data reveal the average trace elements concentration in groundwater is in the following order: Fe > Mn > Sr > Al > Ba > Cr > Zn > Ni > Li > Cu > As > Co > V > Pb > Ag > Pd and the data are presented in the Table 3. The concentrations of palladium (0.001–0.09 g/L), silver (0.001–0.55 g/L), lead (0.001–0.695 g/L), cadmium (0.001–0.10 g/L), chromium (0.30–0.71 g/L), vanadium (0.01–0.83 g/L), aluminium (1.68–32.46 g/L),

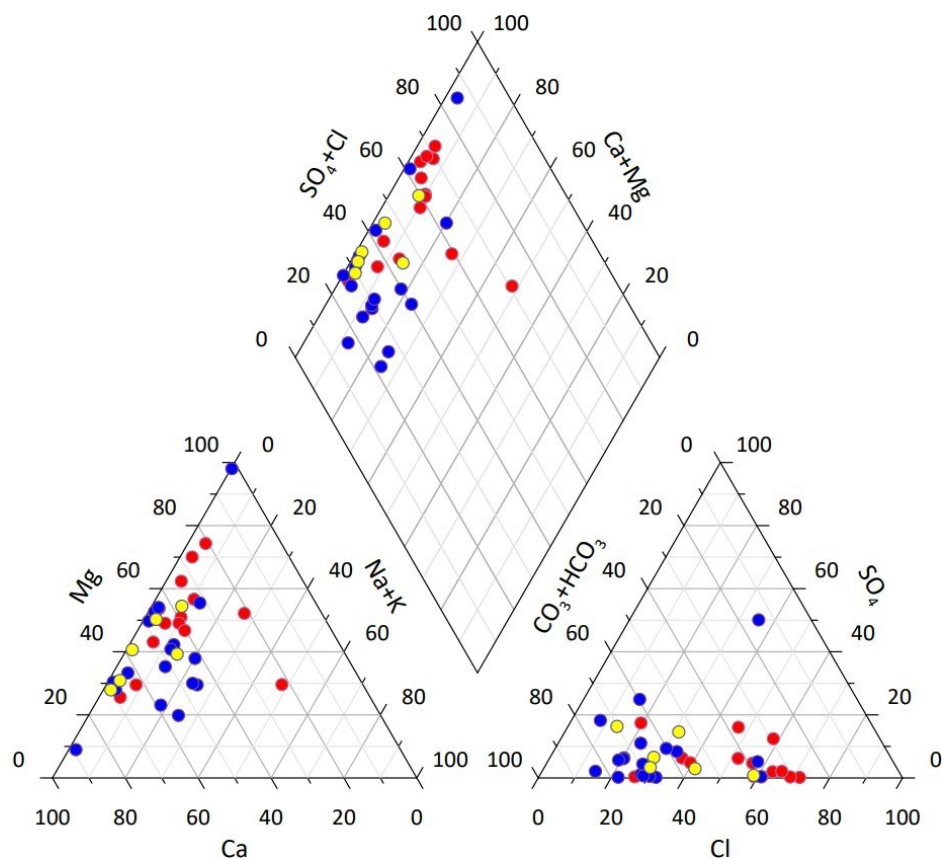


Fig. 4a. Piper plot of groundwater sample.

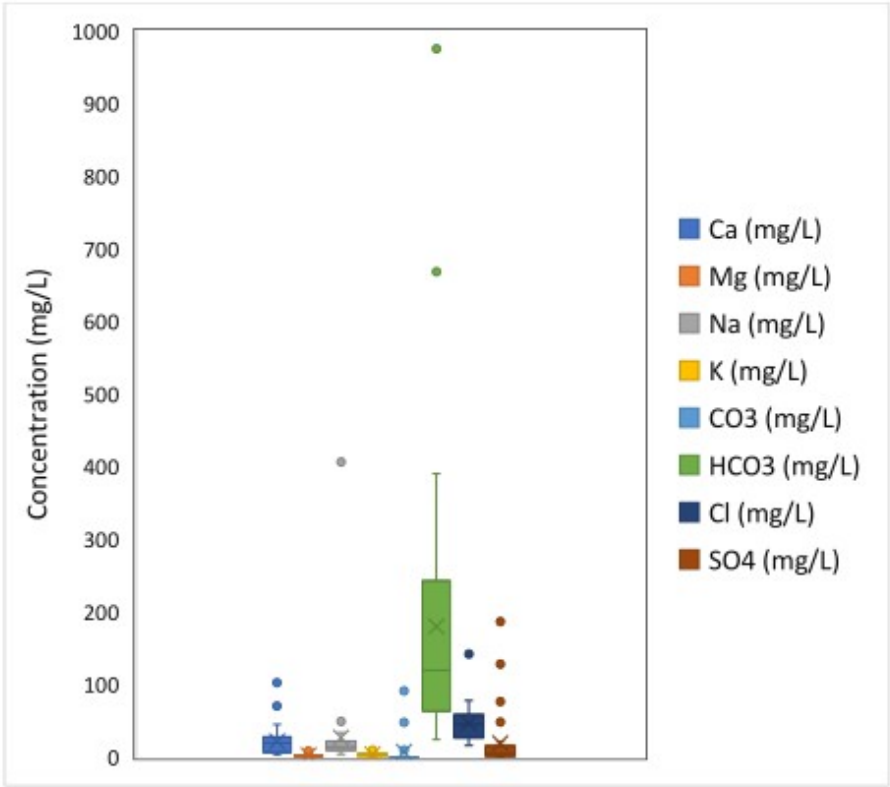


Fig. 4b. Box plot of groundwater sample, which dominated by HCO<sub>3</sub>, Cl and Ca.

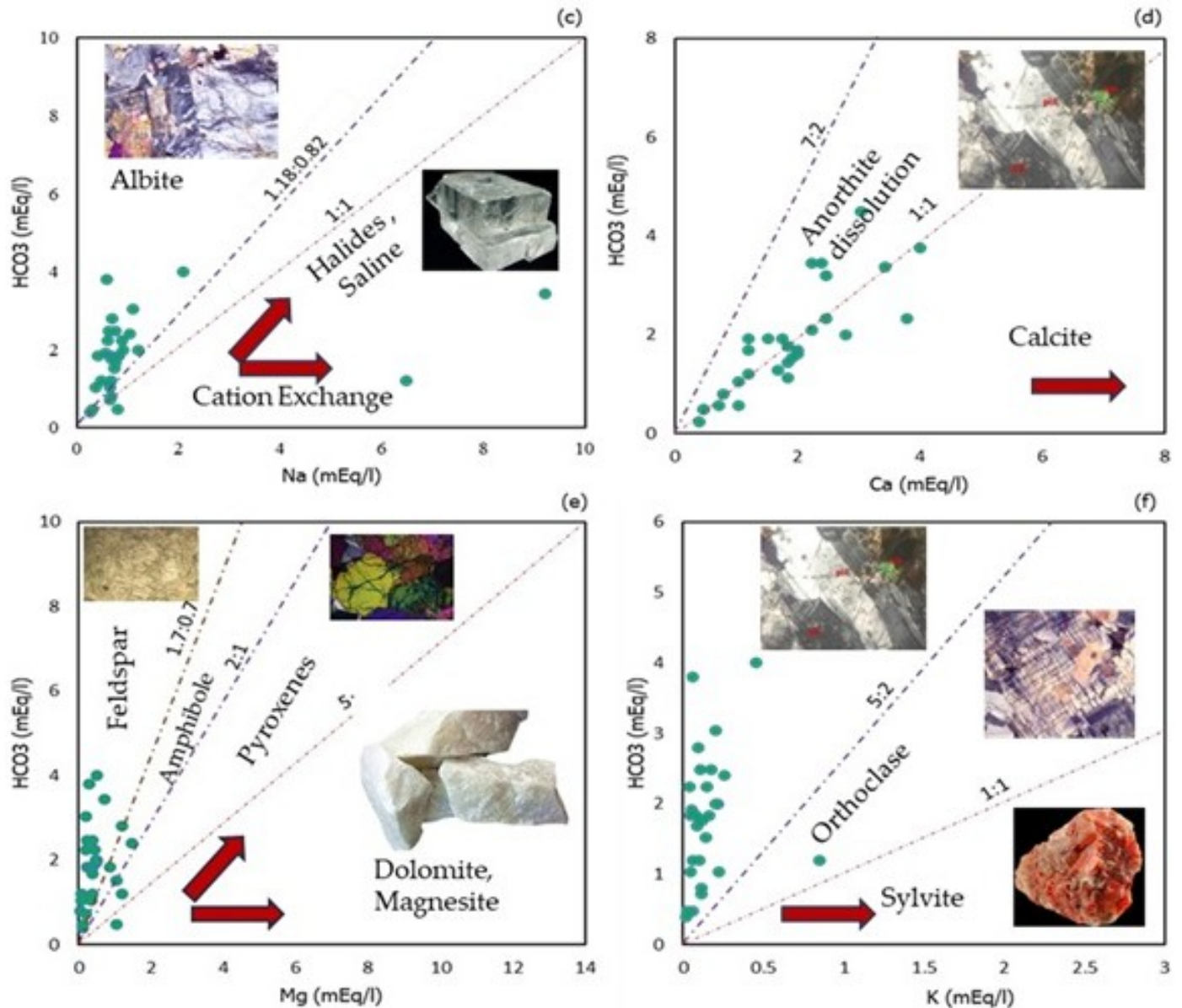


Fig. 4c–f. Shows 1:1 ratio plot (c) HCO<sub>3</sub> vs Na, (d) HCO<sub>3</sub> vs Ca (e) HCO<sub>3</sub> vs Mg (f) HCO<sub>3</sub> vs K. The plots reveal that silicate weathering is the sources for ions in groundwater (Source: Adams et al., 2001; Zhang et al., 2020). Inserted photomicrographs of dolomite and sylvite is taken from web sources.

cobalt (0.30–0.96 g/L), copper (0.18–5.03 g/L), zinc (0.15–21.73 g/L), nickel (0.39–16.11 g/L), lithium (0.02–5.13 g/L), barium (0.69–209.51 g/L), strontium (0.2–1036 g/L), iron (0.54–2952.84 g/L), manganese (0.43–1337.17 g/L) and arsenic (0.01–3.40 g/L) (Table 5). Short description of trace metals in groundwater in NRB is described below.

#### 4.2.1. Chromium (Cr)

Groundwater within regions characterized by ultramafic and mafic rock formations often exhibits elevated Cr concentrations, occasionally surpassing the WHO drinking water guideline of 50 g/L. Cr(VI), a

recognized carcinogen, has prompted increased regulatory analysis due to its toxicity. This study underscores the presence of elevated Cr concentrations in groundwater, ranging from 0.30 to 45.1 g/L. The maximum concentration (45.1 g/L) was observed in deep borewells situated within the Kanthampara area. Fig. 6 illustrates the mechanism by which Cr is released into aqueous solutions. Fig. 7(a) depicts the depth-wise distribution of Cr in NRB. The data reveals that Cr concentrations do not necessarily increase with increasing depth. Over 95% of groundwater samples exhibited Cr concentrations within the range of 0–10 g/L at depths between 5 and 100 m.



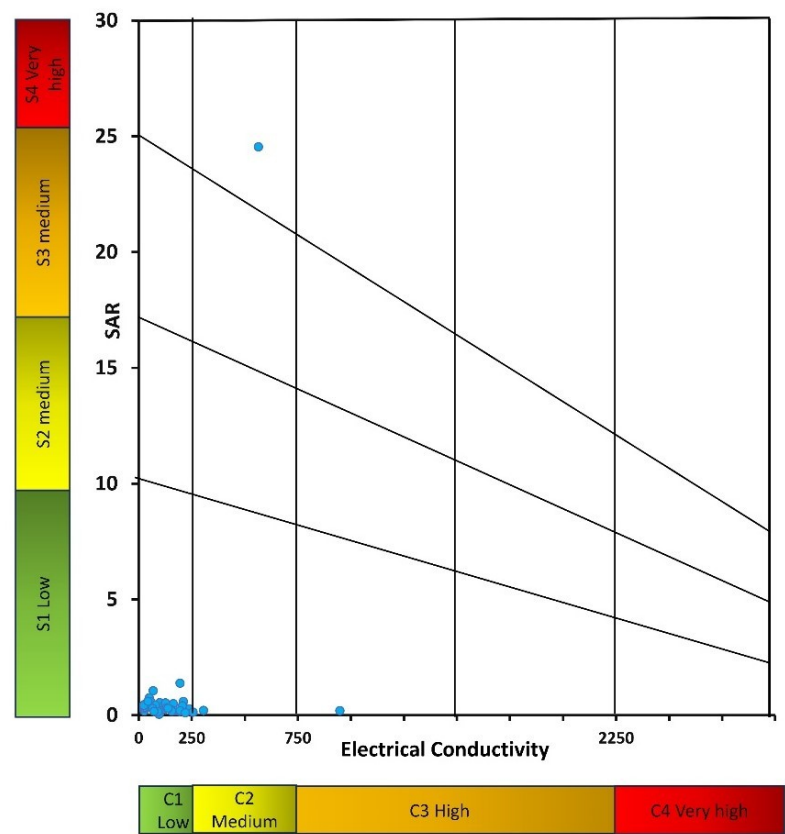


Fig. 4g. USSL salinity diagram of groundwater samples.

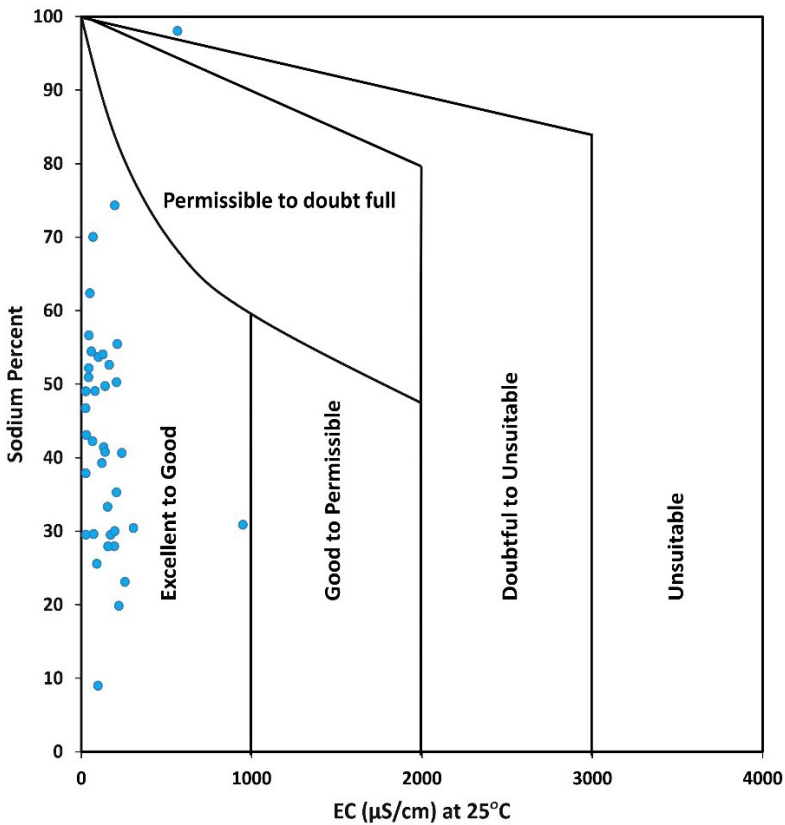


Fig. 4h. Wilcox diagram.

Only two samples exceeded 20 g/L, with one sample reaching a concentration of 45 g/L, approaching the WHO's recommended permissible limit (50 g/L).

#### 4.2.2. Manganese (Mn)

Regular consumption of Mn-contaminated drinking water has been linked to Alzheimer's disease, manganism, and weakness. Anorexia and muscular pain. The presence of Mn in drinking water can cause discolouration. Fig. 7(b) depicts the depth-wise distribution of Mn in NRB. Mn value ranges from 0.43 to 1337.17 µg/L. The data reveals that Mn concentrations do not necessarily increase with increasing depth. Over 95% of groundwater samples exhibited Mn concentrations within the range of 0–100 g/L at depths between 5 and 100 m. Only two sample from Ajanur coastal filter point well exceeds WHO's recommended permissible limit (300 g/L).

#### 4.2.3. Iron (Fe)

Iron, a critical element for human health, can contaminate groundwater in significant quantities. While low levels are necessary, high concentrations cause aesthetic issues such as discolouration, metallic taste, and staining, as well as microbial growth. The World Health Organization's (WHO, 2021) maximum permissible limit for Fe in drinking water is 0.3 mg/L. In 2012, the BIS established a maximum limit of 1000 µg/L for Fe in drinking water. The study area contains significant iron contamination, with some samples exceeding the recommended limit by orders of magnitude. This raises serious concerns about water quality and human health. Fig. 7(c) depicts the depth-wise distribution of Fe in NRB. The Fe values in the study area range between 0.541–2952.848 µg/L. The graph reveals that Fe concentrations increase with increasing depth. Elevated level of Fe occurs only in deep bore well (>80 m). The highest value is obtained from a borewell in Ambalathara.

#### 4.2.4. Arsenic (As)

As in drinking water has a maximum permissible limit of 10 g/L (WHO), regular consumption can cause serious health issues, including cancer. A variety of factors influence release into groundwater, including pH, organic matter content, sediment saturation, and microbial activity. The key mechanisms are as-bearing mineral oxidation and dissolution, organic matter-induced weathering and reductive dissolution, a combination of oxidative and reductive

processes (Shaji et al., 2021). Fig. 7(d) depicts the depth-wise distribution of As in NRB. The As values in the study area range between 0.01–3.40 µg/L. The graph reveals that As concentrations does not increase with increasing depth but enrichment of As is restricted only in shallow depth (0–5 m). The maximum value of As is observed from the Ajanur coastal well.

#### 4.2.5. Strontium (Sr)

Groundwater with excess Sr is derived from carbonates and evaporite sedimentary aquifers, but in silicate (hard rock) aquifers, Sr in groundwater is controlled by leaching via the rock water interaction process (Sarath et al., 2023). WHO does not set a limit for Sr in drinking water, but recommends a health reference value of 1500 g/L (USEPA, 2014). Sr can stimulate bone growth while also preventing and treating osteoporosis (Alexandersen et al., 2011; Shin et al., 2021). High-level Sr consumption is harmful to health because its bone calcification (Langley et al., 2009). Fig. 7(e) depicts the depth-wise distribution of Sr in NRB. The Sr values in the study area range between 0.21–1036 µg/L. The graph reveals that As concentrations does not increase with increasing depth but the maximum Sr is observed from a filter point well of Ajanur coastal area.

#### 4.2.6. Barium (Ba)

The WHO maximum allowable limit for Ba is 0.7 mg/L. Long-term ingestion of high doses of barium can harm the kidneys and has been linked to cardiovascular problems (Dallas and Williams, 2001; Peana et al., 2021). Ba in groundwater is produced by the weathering and dissolution of evaporates and celsian feldspar minerals. No sample exceeds the permissible limit. Fig. 7(f) depicts the depth-wise distribution of Ba in NRB. Ba concentrations in the study area range from 0.69 to 209.51 µg/L. The graph reveals that Ba concentrations does not increase with increasing depth but the amount of Ba is increased in coastal and deep bore well but do not exceeding the maximum permissible limit of WHO and BIS.

#### 4.2.7. Nickel (Ni)

Humans are susceptible to a wide range of adverse health effects resulting from exposure to environments with elevated nickel (Ni) concentrations. The International Agency for Research on Cancer classifies nickel compounds as human carcinogens, particularly associated with cancers of the lung, nasal

cavity, and paranasal sinuses following inhalation exposure. Natural sources of Ni in the atmosphere include wind-borne dust from rock and soil weathering, volcanic emissions, forest fires, and the release of Ni from vegetation. Anthropogenic sources of atmospheric Ni include the combustion of coal, diesel oil, and fuel oil, as well as the incineration of waste and sewage. Fig. 7(g) depicts the depth-wise distribution of Ni in groundwater within the NRB region. The data does not indicate any significant enrichment of Ni in groundwater with increasing depth. Only one sample, originating from a borewell in Meengoth, exhibited the maximum Ni concentration of 16 µg/L. WHO has established a guideline value of 20 µg/L for Ni in drinking water. No samples exceeded this limit.

#### 4.2.8. Aluminum (Al)

Regular consumption of water contaminated with aluminum (Al) can have significant adverse health consequences, including Alzheimer's disease, nausea, vomiting, diarrhea, mouth and skin ulcers, skin rashes, and arthritis pain. The WHO has established a guideline value of 200 µg/L for Al in drinking water. Al concentrations in the NRB region were observed to range from 1.68 to 32.46 µg/L. According to the Bureau of Indian Standards (BIS), the desirable limit for Al in drinking water is 30 µg/L. Only one sample, originating from a borewell in Meengoth, exceeded this limit. Fig. 7(h) illustrates the depth-wise distribution of Al in NRB groundwater, the graph indicates that a significant enrichment of Al occurs primarily in deep borewell samples. In shallower depths, Al concentrations in most samples fall within the range of 0–10 µg/L. A slight increase in Al concentrations is observed with increasing well depth. Two lateritic dug wells exceeding 20 m in depth exhibit Al concentrations greater than 20 µg/L. According to BIS, the desirable limit for Al in drinking water is 30 µg/L. Only one sample from a borewell in Meengoth exceeded this limit.

#### 4.2.9. Palladium (Pd)

Groundwater has been identified as a valuable medium for geochemical exploration of various mineralisation styles, including PGEs and gold (Narayanaswamy et al., 1998). The concept is based on groundwater interaction with the mineralised zone, as well as trace/heavy metal leaching at optimal pH-Eh conditions. In comparison to surface geo-

chemical methods, subsurface groundwater recharge increases the likelihood of rock-water interaction with buried mineralisation (Balaram et al., 2019). PGEs, which are also emitted by vehicle exhaust catalysts, have accumulated significantly in environmental matrices over the last few decades. It is still debated whether the emitted PGEs are harmful to living organisms and humans. Pd levels in NRB range from 0.001–0.09 g/L, with the highest concentration observed in the Ajanur coastal well (Fig. 8a).

#### 4.2.10. Vanadium (V)

V is a necessary trace element, but it can be harmful at higher concentrations. Industrial activities, particularly oil refining and coal-fired power plants, are significant sources of environmental V. High dissolved V levels in surface waters may indicate oil pollution, whereas groundwater V concentrations reflect the type of rock being weathered. V is more common in mafic rocks like basalt and gabbro than in silicic rocks like granite. Shale, particularly marine shale rich in organic carbon, can have a high V content. While V has some medicinal applications, excessive exposure can cause respiratory irritation, cardiovascular issues, and neurological damage. V in NRB ranges from 0.01–0.83 g/L (Fig. 8a).

#### 4.2.11. Cadmium (Cd)

Cadmium is a toxic metal that occurs naturally in the environment and as a pollutant from industrial and agricultural sources. Cd is a nephrotoxic metal that damages kidney tubules and bones. Cd is found in groundwater as a result of rock-water interactions. The Cd concentration in the study area ranges from 0.001 to 0.102 µg/L (Fig. 8a). Cd levels should not exceed 3 µg/L, according to WHO guidelines. No sample has exceeded the permissible limit.

#### 4.2.12. Lead (Pb)

WHO classifies lead as one of ten chemicals of major concern for public health and one of the most dangerous environmental poisons. The WHO's lead guideline value of 10 µg/L is no longer considered a health-based value and has been designated as provisional (Jarvis and Fawell, 2021). Pb concentrations in the NRB vary from 0.001–0.69 µg/L (Fig. 8a). No sample exceeds the maximum permissible limit.

#### 4.2.13. Silver (Ag)

Silver is rarely found in high concentrations in drinking water. Silver concentrations in surface



water and groundwater are typically below 2 µg/L (ATSDR, 2000). The only known clinical picture of chronic silver intoxication is argyria, a condition in which silver is deposited in the skin, hair, and organs as a result of occupational or iatrogenic exposure to metallic silver and its compounds (WHO, 2021). Silver concentrations in natural waters typically range between 0.2 and 0.3 µg/L (United States Environmental Protection Agency, 1980). The toxicological database on silver is inadequate to support the development of a formal guideline value. Ag concentrations in the NRB range from 0.001–0.55 µg/L (Fig. 8a).

#### 4.2.14. Lithium (Li)

Granites and pegmatites contain lithium minerals. Lindsey et al. (2021) classified Li as a potential threat to human health. A meta-analysis of clinical trials (Cipriani et al., 2013) found that Li is an effective treatment for reducing suicidal ideation in people with mental health issues. The WHO does not recommend a lithium guideline value for drinking water. Li concentrations in NRB range between 0.02 and 5.13 µg/L. The highest lithium value is found at a shallow filter point on the Ajanur coast (Fig. 8b).

#### 4.2.15. Copper (Cu)

Cu in water undergoes a number of transformations depending on pH, oxygen levels, and the presence of other substances. It first oxidises to Cu(I), which is then oxidised to Cu(II) in most cases. However, certain copper(I) complexes can be stable. Cu(II) forms complexes with hydroxide and carbonate ions, and malachite is an important insoluble compound. Cu is primarily present in water as the Cu(II) ion, and its speciation varies with pH. Cu concentrations in drinking water vary greatly due to differences in water properties such as pH, hardness, and copper availability in the distribution system. Cu ions can produce symptoms similar to food poisoning (headache, nausea, vomiting, and diarrhoea). The WHO guideline value for Cu is 2 mg/L. BIS value of Cu for drinking water is 50 µg/L to 1500 µg/L. Cu value of NRB is ranges from 0.18–5.03 µg/L and maximum value observed from a bore well from Meenagoth. No samples exceed maximum permissible limit (Fig. 8b).

#### 4.2.16. Zinc (Zn)

Zinc is an essential element whose importance to health is increasingly recognised. Zinc deficiency

causes growth retardation, hypogonadism, immune dysfunction, and cognitive impairment in nearly two billion people in the developing world. The BIS acceptable limit for Zn in drinking water is 5 mg/L, while the maximum limit is 15 mg/L. Zn concentrations in NRB range from 0.15 to 21.73 µg/L (Fig. 8b). Geologically, Zn is primarily associated with sulphide minerals. The highest Zn concentration is found in the Parakalayi area.

### 4.3. Groundwater quality for irrigation purposes

Water quality for irrigation is critical for the extent of vegetable cover, soil productivity, and environmental protection. Irrigation water containing an excess dissolved ions has a negative impact on both plants and soil, both physically and chemically. The composition and constituents of dissolved salts in groundwater determine whether or not the water is suitable for irrigation. Groundwater irrigation suitability is determined using USSL and Wilcox diagrams.

#### 4.3.1. USSL Diagram

The US Salinity Laboratory Diagram (USSL) is a tool used to assess irrigation water quality based on sodium adsorption ratio (SAR) and electrical conductivity (EC). It classifies water into 16 zones, each representing a specific level of sodium and salinity hazard.

In the study area, most groundwater samples fell into the C1S1 category, indicating low salinity and sodium hazard, making them suitable for irrigation. A small percentage of samples were categorized as C2S1 (medium salinity) and one sample as C3S1 (high salinity), suggesting potential issues for certain crops (Fig. 4g). Overall, the groundwater quality in the study area is considered good for irrigation purposes.

#### 4.3.2. Wilcox diagram

The Wilcox diagram is a tool used to assess the suitability of irrigation water based on sodium percentage (Na%) and electrical conductivity (EC). It divides water into five zones, ranging from excellent to unsuitable quality. Based on the Wilcox diagram, most of the groundwater samples in the study area fall into the “excellent to good” category, indicating that they are suitable for irrigation. Only a few samples were close to the “good to permissible” category. Overall, the groundwater in the study area has a low

sodium percentage and is generally suitable for irrigation (Fig. 4h).

#### 4.4. Petrography & Whole-rock geochemistry

The rock charnockite is a medium-grained, hard, and heavy rock with a greasy appearance. It primarily consists of quartz, feldspar, and pyroxenes (Fig. 5a–c). Lodestone, a type of vanadiferous-magnetite deposit. It forms through magmatic processes and subsequent alteration. Based on the petrographical observation (Fig. 5d–f) lodestone exhibits a polycrystalline granular texture with euhedral and subhedral magnetite grains. Martitization, a low-temperature oxidation process, affects the grain boundaries of magnetite. Ilmenite occurs in various forms: individual grains, blebs within magnetite, fracture fillings, and intergrowths with hematite. Paragenesis of lodestone involves three stages: Magnetite replacement by ilmenite, ilmenite replacement by hematite finally hematite replacement by goethite (Sukumaran and Nambiar, 2001). Pyroxene granulites exhibit a granoblastic texture with non-foliated minerals, resulting in a lack of strong schistosity. They are typically composed of plagioclase feldspar and pyroxene (Fig. 5g–i).

The XRF data of rocks, detailing major oxides are provided in Table 6. Major oxide concentration in meta-pyroxenite is following order  $\text{SiO}_2 > \text{MgO} > \text{Fe}_2\text{O}_3 > \text{CaO} > \text{Al}_2\text{O}_3$ . Pyroxene Granulite  $\text{SiO}_2 > \text{Fe}_2\text{O}_3 > \text{Al}_2\text{O}_3 > \text{CaO} > \text{MgO} > \text{Na}_2\text{O}$ . Charnockite is following order  $\text{SiO}_2 > \text{Al}_2\text{O}_3 > \text{CaO} > \text{Fe}_2\text{O}_3 > \text{MgO}$ .

## 5. Discussion

A detailed hydrogeological field investigation is carried out entire area of NRB and identified that the people facing groundwater shortage in the pre-monsoon season especially February to May. Rapid decline of groundwater level in the phreatic aquifer of lateritic terrain due to highly porous nature of the rock is major threat. Thick, dense duricrust layer also a burden in monsoon and post monsoon which effect non recharge of rainwater. A comprehensive analysis of major ions and trace metals was conducted in groundwater samples from various depths in the NRB aquifer system. Hydrogeochemical analysis provided an insight into the relationships between various water quality parameters in the KRB region. As water depth increases, the pH becomes more alkaline.

Nitrate levels are negatively related to  $\text{PO}_4$ ,  $\text{SO}_4$ , and Li, indicating a geogenic origin from silicate rock weathering. The low levels of anthropogenic contaminants like Cl, Na,  $\text{NO}_3$ ,  $\text{PO}_4$ , and  $\text{SO}_4$  suggest that natural geological processes are the primary drivers of water quality.

The study area's hydrogeochemical facies were predominantly  $\text{Ca}^{2+}\text{--Mg}^{2+}\text{--HCO}_3^-$  with Temporary Hardness water type, except for two samples from bore wells of Banam and Malpacherry. Alkaline earth metals (Ca, Mg, Sr, and Ba) slightly predominate over alkali metals (Na, K, and Li) in groundwater, while weak acids ( $\text{HCO}_3$ ) exceed strong acids (Cl and  $\text{SO}_4$ ). The hydrogeochemistry of hard crystalline terrains is complex due to distinct geological and hydrogeological properties. The slow weathering of silicate minerals, minimal soil profile thickness, and lack of residence time for rock water interaction control hydrogeochemical facies and evolving water types. Cation exchange processes and the mixing of young and old groundwater in fractures distort expected ion ratios, contributing to ionic balance errors.

Fig. 7(a–h) shows depth wise distribution of some of the selected trace metals in NRB such as depth  $v/s$  Cr, Mn, Fe, As, Sr, Ba, Ni and Al respectively. Fe exceeds the both BIS 2012, and WHO, 2022 maximum permissible limits for drinking water purposes. Enrichment of Fe and Cr in deep (>80 m) groundwater resources especially in Kanthampara area, which consists of ultramafic rocks like lodestone and pyroxenites in aquifer lithounits. Decomposition of the organic matter in shallow depth depletes the oxygen in the water and often accompanied by dissolved Mn. When this water is pumped to the surface, the dissolved Mn form blackish particulates in the water. Elevated level of Mn is overserved in the filter point wells of Ajanur coastal area at depth of 5 m (see Fig. 7b). As, Sr and Ba is also observed in the shallow depth (4–10 m) at Ajanur coastal area. Percolation of these light weight metals in to deep groundwater resources is limited or saline environment play crucial role for the abundance of these particular elements, but none of the samples exceeds the maximum permissible limits. Concentration of Ni and Al restricted in to deep bore wells only. Ni were observed from Kanthampara region at depth of 100 m.

The northeastern part, characterized by deep aquifers in the highlands of the Western Ghats, is dominated by Fe and Cr, along with other trace metals. The central part of the NRB, characterized by



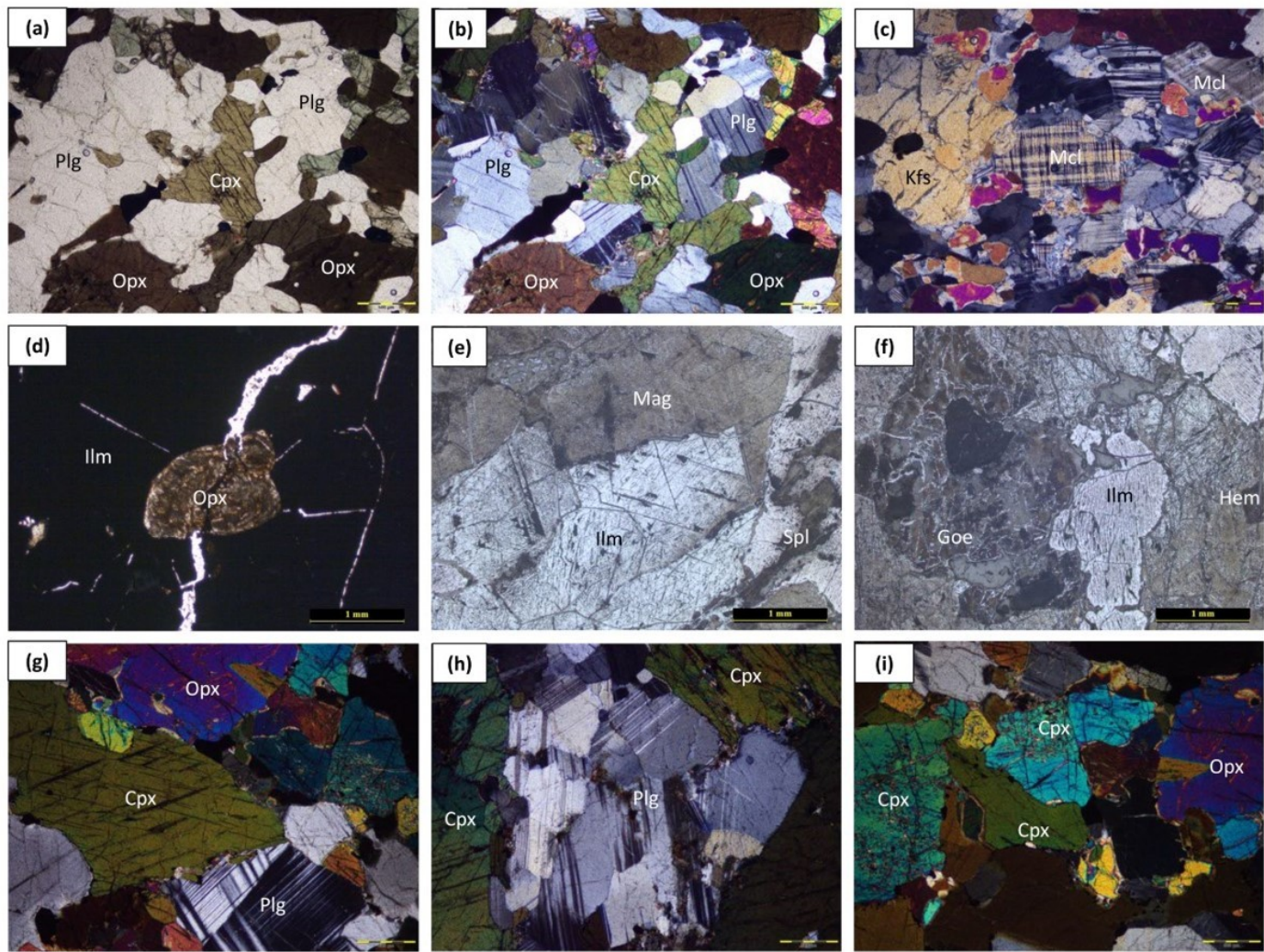


Fig. 5. (a–i). Photomicrographs showing representative minerals in mafic and ultramafic rocks from Kanthampara area. (a–c) Charnockite basement rocks contain pyroxenes, feldspars (plagioclase, microcline), and opaque minerals (d–f) lodestone shows opaque grains and opx grain, silicates can be observed along the fractures, transformation of magnetite to ilmenite, hematite and goethite is noticed.

Table 6. XRF data of the rock types of the study area.

Sample No.	Sample	SiO <sub>2</sub>	TiO <sub>2</sub>	Al <sub>2</sub> O <sub>3</sub>	MnO	Fe <sub>2</sub> O <sub>3</sub>	CaO	MgO	Na <sub>2</sub> O	K <sub>2</sub> O	P <sub>2</sub> O <sub>5</sub>
1	Metapyroxenite	46.1	0.66	8.71	0.2	14	9.96	17.8	1.51	0.54	0.13
2	Pyroxene Granulite	46.73	1.88	12.34	0.24	21.79	7.17	5.98	3.34	0.21	0.22
3	Charnockite	68.62	0.29	16.92	0.02	2.6	4.44	1.07	5	0.79	0.08

flat lateritic terrain, wells in both regions are safe for drinking water purposes. In contrast, the southwestern part, comprising sedimentary depositional environments, exhibits enrichment in major ions in few wells, especially Na and Cl due to coastal activity.

Overall, the NRB comes under a drought prone area in pre-monsoon season (February to May). A micro level studies are recommended to overcome the groundwater scarcity condition and Fe identification and mitigation. Artificial recharge techniques like percolation tanks, stream augmentation, LDPE pond

lining have been suggested in the study area based on drainage density.

6. Conclusion

Groundwater is an important source for various uses in the Nileshwaram river basin. This paper investigated the major ion and trace elements chemistry of groundwater in the area with various methods such as detailed geological field investigations, petrographical, geochemical and statistical analysis. The water quality for agricultural and drinking purposes



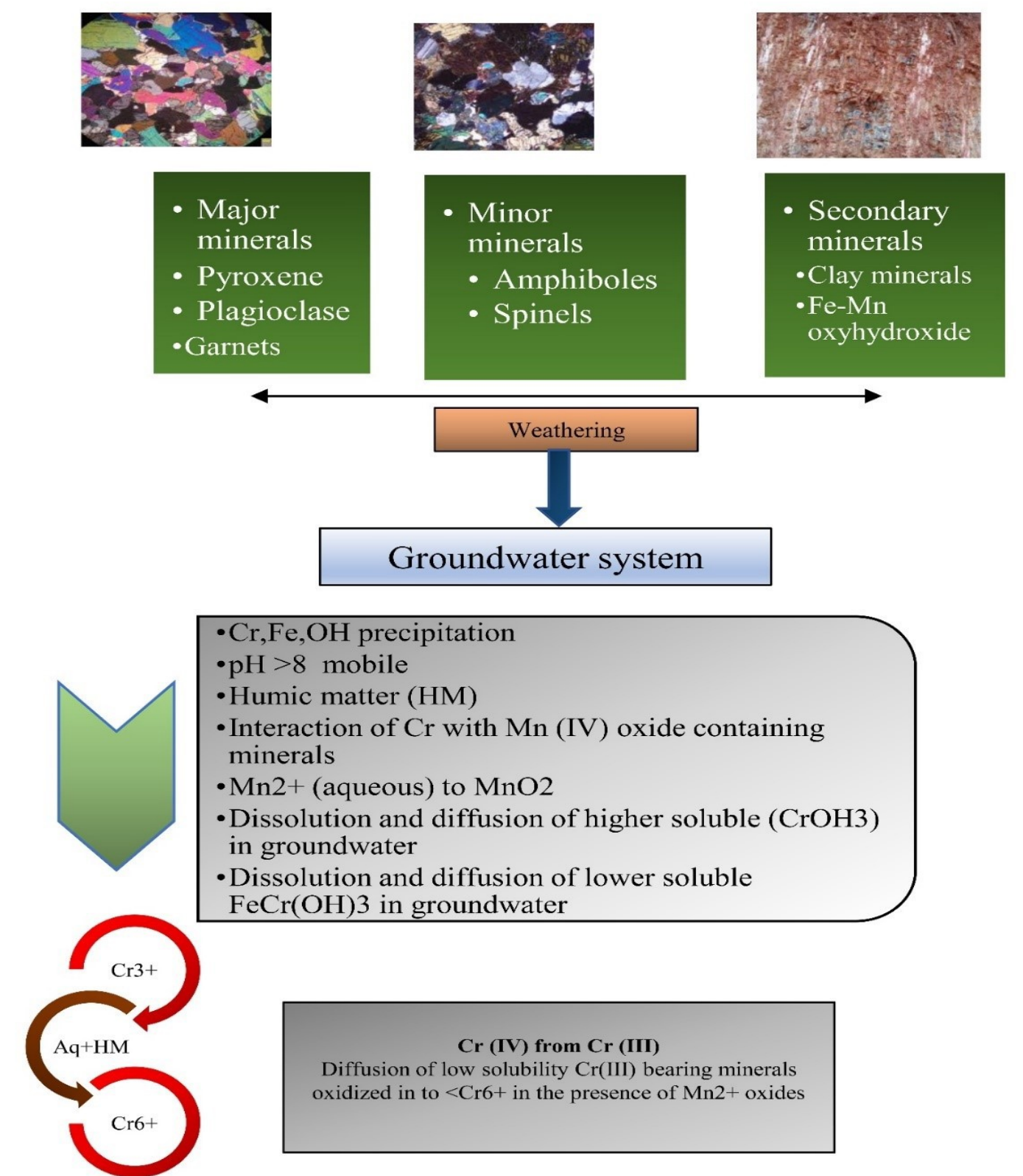


Fig. 6. Release mechanism of Cr into aqueous solution. Modified after Chrysochoou et al. (2016), Hausladen and Fendorf (2017), Tumolo et al. (2020)..

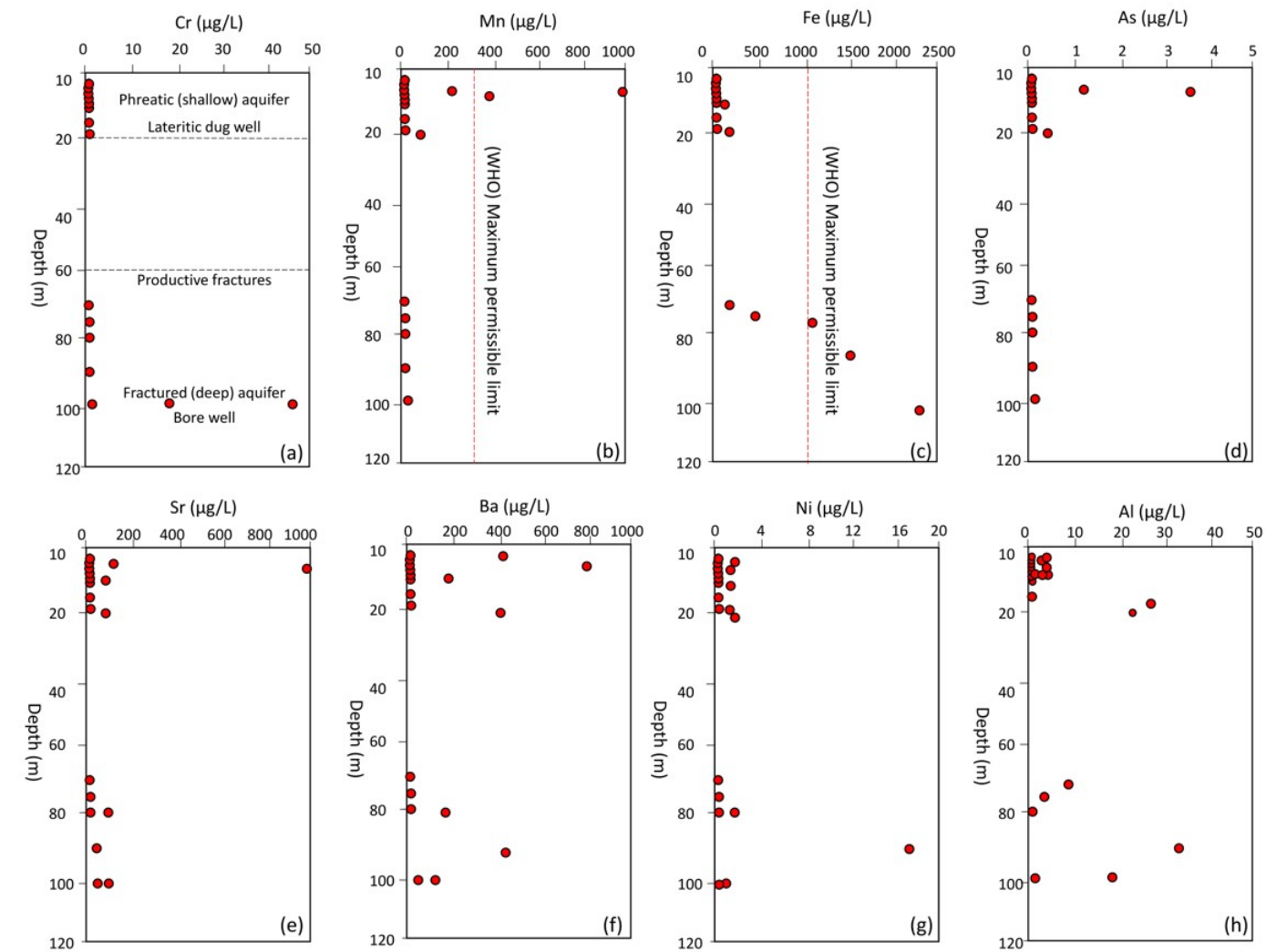


Fig. 7. Depth wise distribution of selected trace metals in NRB such as Cr, Mn, Fe, As, Sr, Ba, Ni and Al.

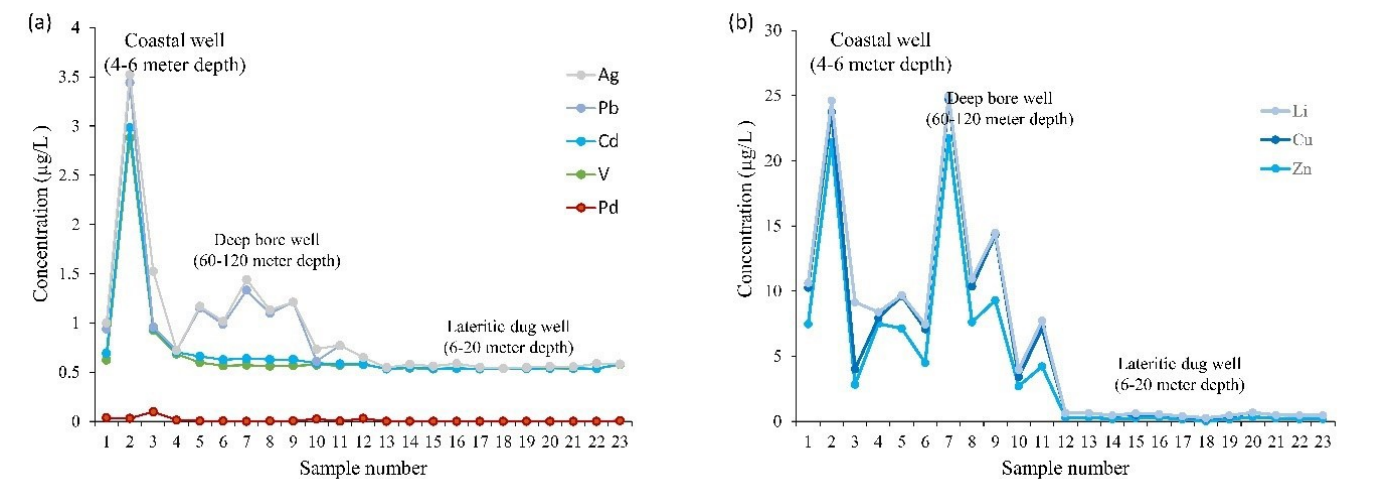


Fig. 8. (a) Shows the distribution of Pd, V, Cd, Pb and Ag (b) Zn, Cu, and Li in groundwater, respectively.

was also assessed. The following conclusions can be reached.

- The concentrations of major cations and anions were low in the groundwater in the area, indicating good water quality. The concentrations of major chemical parameters were relatively higher near coastal area than in other areas. The hydrochemical facies of groundwater in the study area are dominantly  $\text{HCO}_3\text{--Ca}$  types.
- Alkaline earth metals (Ca, Mg, Sr, and Ba) slightly predominate over alkali metals (Na, K, and Li) in the groundwater.
- The hydrogeochemistry of hard crystalline terrains is complex due to distinct geological and hydrogeological properties. Geochemical processes are driven by the slow weathering of silicate minerals such as feldspar, biotite, and hornblende.
- All major ions were within India's desirable limits for water quality and the desirable permissible limits of the WHO.
- Field evidence supports silicate weathering, ruled out the dissolution of halides and calcite.
- Groundwater quality in the study area, revealed by Wilcox, and USSL diagrams, is generally suitable for agricultural use, with low alkalinity, total hardness but medium salinity. The concentrations of the main chemical parameters suggest that groundwater in the study area is fit for human consumption.
- The groundwater of NRB is controlled by weathering of rock-forming minerals. This is confirmed by the results of whole rock geochemical and petrographical analysis. The main hydrogeochemical processes include the dissolution of feldspar group of minerals and ferromagnesian minerals, and no role for precipitation of halite, gypsum, calcite, and dolomite.
- Distribution of trace elements concentration in groundwater is in the following order:  $\text{Fe} > \text{Mn} > \text{Sr} > \text{Al} > \text{Ba} > \text{Cr} > \text{Zn} > \text{Ni} > \text{Li} > \text{Cu} > \text{As} > \text{Co} > \text{V} > \text{Pb} > \text{Ag} > \text{Pd}$ . Only Fe and Mn exceeds the WHO and BIS maximum permissible limits.

- The northeastern part of the NRB is prone to drought, with deep aquifers dominated by Fe and anomalous value of Mn and Cr. The central part has safe drinking water, while the southwestern part exhibits ion enrichment due to coastal activity. Micro-level studies and artificial recharge techniques are recommended.

### CRediT authorship contribution statement

**KVS:** Conceptualization, Investigation, Methodology, Data generation, Writing – review & editing, corresponding author. **NA:** Investigation, Data generation, Writing – review & editing. **AA:** Writing – original draft, Writing – review & editing. **VN:** Investigation, Writing – review & editing. **ES:** Writing – review, editing, supervision.

### Declaration of competing interest

The authors declare that they have no known competing financial interests or personal relationships that could have appeared to influence the work reported in this paper.

### Acknowledgments

Authors are thankful to IUAC for extending Q-ICPMS established under the National Geochronology Facility funded by the Ministry of Earth Science (MoES) with the project reference number MoES/P.O. (Seismic)8(09)-Geochron/2012. Director, NCESS, Thiruvananthapuram is thanked for the thin section, and XRF facilities. The authors thank KSCSTE, Govt. of Kerala for providing fellowship to the first author under the arsenic project (No KSCSTE/ 5979/2017-E&E). Dr. Sandeep K, Kommu Sandeep and Arya B K of Central University of Kerala, India are thanked for the support during field studies.

### References

- Adams, S., Titus, R., Pietersen, K., Tredoux, G., Harris, C., 2001. Hydrochemical characteristics of aquifers near Sutherland in the Western Karoo, South Africa. *Journal of Hydrology* 241(1–2), 91–103. [https://doi.org/10.1016/S0022-1694\(00\)00370-X](https://doi.org/10.1016/S0022-1694(00)00370-X).
- Alexandersen, P., Karsdal, M.A., Byrjalsen, I., Christiansen, C., 2011. Strontium ranelate effect in postmenopausal women with different clinical levels of osteoarthritis. *Climacteric* 14(2), 236–243. <https://doi.org/10.3109/13697137.2010.507887>.



- ATSDR, T., 2000. ATSDR (Agency for Toxic Substances and Disease Registry). *Prepared by Clement International Corp., under contract* 205, 88–0608.
- Balaram, V., Satyanarayanan, M., Anabarasu, K., Rao, D.V.S., Ali, M.D., Kamala, C.T., Charan, S.N., 2019. Hydro-geochemistry as a tool for platinum group element (PGE) exploration—A case study from Sittampundi Anorthosite Complex, southern India. *Journal of the Geological Society of India* 94(4), 341–350. <https://doi.org/10.1007/s12594-019-1321-7>.
- Barbier, E., 2019. *The Water Paradox: Overcoming the Global Crisis in Water Management*. Yale University Press.
- Bhatnagar, I., Dhanya, C.T., Chahar, B.R., 2024. Do groundwater systems experience a 'silent' stress? A paradox of rising groundwater levels and stressed aquifers. *Groundwater for Sustainable Development* 25, 101111. <https://doi.org/10.1016/j.gsd.2024.101111>.
- Chandra, P.C., 2015. *Groundwater Geophysics in Hard Rock*. CRC press.
- Chrysoschoou, M., Theologou, E., Bompoti, N., 2016. Occurrence, origin and transformation processes of geogenic chromium in soils and sediments. *Curr Pollution Rep* 2, 224–235. <https://doi.org/10.1007/s40726-016-0044-2>.
- Cipriani, A., Hawton, K., Stockton, S., Geddes, J.R., 2013. Lithium in the prevention of suicide in mood disorders: updated systematic review and meta-analysis. *BMJ* 346. <https://doi.org/10.1136/bmj.f3646>.
- Dallas, C.E., Williams, P.L., 2001. Barium: rationale for a new oral reference dose. *Journal of Toxicology and Environmental Health Part B: Critical Reviews* 4(4), 395–429. <https://doi.org/10.1080/109374001753146216>.
- Gleeson, T., Vander Steen, J., Sophocleous, M.A., Taniguchi, M., Alley, W.M., Allen, D.M., Zhou, Y., 2010. Groundwater sustainability strategies. *Nature Geoscience* 3(6), 378–379. <https://doi.org/10.1038/ngeo881>.
- Hanasaki, N., Yoshikawa, S., Pokhrel, Y., Kanae, S., 2018. A global hydrological simulation to specify the sources of water used by humans. *Hydrology and Earth System Sciences* 22(1), 789–817. <https://doi.org/10.5194/hess-22-789-2018>.
- Hausladen, D.M., Fendorf, S., 2017. Hexavalent chromium generation within naturally structured soils and sediments. *Environmental Science & Technology* 51(4), 2058–2067. <https://doi.org/10.1021/acs.est.6b04039>.
- Hurtado, A.R., Díaz-Cano, E., Berbel, J., 2024. The paradox of success: Water resources closure in Axarquía (southern Spain). *Science of the Total Environment* 946, 174318. <https://doi.org/10.1016/2024.174318>.
- Jarvis, P., Fawell, J., 2021. Lead in drinking water—an ongoing public health concern? *Current Opinion in Environmental Science & Health* 20, 100239. <https://doi.org/10.1016/j.coesh.2021.100239>.
- Konikow, L.F., Kendy, E., 2005. Groundwater depletion: A global problem. *Hydrogeology Journal* 13, 317–320. <https://doi.org/10.1007/s10040-004-0411-8>.
- Kuang, X., Liu, J., Scanlon, B.R., Jiao, J.J., Jasechko, S., Lancina, M., Zheng, C., 2024. The changing nature of groundwater in the global water cycle. *Science* 383(6686), 0630. <https://doi.org/10.1126/science.adf0630>.
- Langley, S., Gault, A.G., Ibrahim, A., Takahashi, Y., Renaud, R., Fortin, D., Clark, I.D., Ferris, F.G., 2009. Sorption of strontium onto bacteriogenic iron oxides. *Environmental Science & Technology* 43(4), 1008–1014. <https://doi.org/10.1021/es802027f>.
- Lindsey, B.D., Belitz, K., Cravotta III, C.A., Tocalino, P.L., Dubrovsky, N.M., 2021. Lithium in groundwater used for drinking-water supply in the United States. *Science of the Total Environment* 767, 144691. <https://doi.org/10.1016/j.scitotenv.2020.144691>.
- Maliva, R.G., 2020. Geochemistry and managed aquifer recharge basics. *Anthropogenic Aquifer Recharge: WSP Methods in Water Resources Evaluation Series No. 5*, 103–131. [https://doi.org/10.1007/978-3-030-11084-0\\_5](https://doi.org/10.1007/978-3-030-11084-0_5).
- Mays, L.W., 2013. Groundwater resources sustainability: past, present, and future. *Water Resources Management* 27, 4409–4424. <https://doi.org/10.1007/s11269-013-0436-7>.
- Munir, M.U., Blaurock, K., Frei, S., 2024. Understanding the vulnerability of surface-groundwater interactions to climate change: insights from a Bavarian Forest headwater catchment. *Environmental Earth Sciences* 83(1), 12. <https://doi.org/10.1007/s12665-023-11314-2>.
- Narayanaswamy, Balaram, V., Ramkumar, N., Anjaiah, K.V., 1998. Concentration of gold in natural waters from lateritic terrain, Wynad-Nilambur Gold Field, Kerala, India and its possible role in exploration. *Journal Geological Society of India* 52(3), 301–304. <https://doi.org/10.17491/jgsi/1998/520306>.
- Peana, M., Medici, S., Dadar, M., Zoroddu, M.A., Pelucelli, A., Chasapis, C.T., Bjørklund, G., 2021. Environmental barium: potential exposure and health-hazards. *Archives of Toxicology* 95(8), 2605–2612. <https://doi.org/10.1007/s00204-021-03049-5>.
- Polya, D.A., Sparrenbom, C., Datta, S., Guo, H., 2019. Groundwater arsenic biogeochemistry—Key questions and use of tracers to understand arsenic-prone groundwater systems. *Geoscience Frontiers* 10(5), 1635–1641. <https://doi.org/10.1016/j.gsf.2019.05.004>.
- Sarath, K.V., Shaji, E., Nandakumar, V., 2023. Characterization of trace and heavy metal concentration in groundwater: A case study from a tropical river basin of southern India. *Chemosphere* 338, 139498. <https://doi.org/10.1016/j.chemosphere.2023.139498>.
- Shaji, E., Santosh, M., Sarath, K.V., Prakash, P., Deepchand, V., Divya, B.V., 2021. Arsenic contamination of groundwater: A global synopsis with focus on the Indian Peninsula. *Geoscience Frontiers* 12(3), 101079. <https://doi.org/10.1016/j.gsf.2020.08.015>.
- Shaji, E., Sarath, K.V., Santosh, M., Krishnaprasad, P.K., Arya, B.K., Babu, M.S., 2024. Fluoride contamination in groundwater: A global review of the status, processes, challenges, and remedial measures. *Geoscience Frontiers* 15(2), 101734. <https://doi.org/10.1016/j.gsf.2023.101734>.
- Shin, W.J., Ryu, J.S., Kim, R.H., Min, J.S., 2021. First strontium isotope map of groundwater in South Korea: applications for identifying the geographical origin. *Geosciences Journal* 25, 173–181. <https://doi.org/10.1007/s12303-020-0013-z>.
- Sophocleous, M., 2004. Global and regional water availability and demand: prospects for the future. *Natural Resources Research* 13, 61–75. <https://doi.org/10.1023/B:NARR.0000032644.16734.f5>.
- Stone, A., Lanzoni, M., Smedley, P., 2019. Groundwater resources: Past, present, and future, in: *Water Science, Policy, and Management: A Global Challenge*, p. 29–54.

- <https://doi.org/10.1002/9781119520627.ch3>.
- Sukumaran, P.V., Nambiar, A.R., 2001. Occurrence of chromiferous lodestone near Chalingal, Kasaragod District, Kerala. *J. Geological Society of India* 58(2), 171–173.
- Taucare, M., Viguiet, B., Figueroa, R., Daniele, L., 2024. The alarming state of Central Chile's groundwater resources: A paradigmatic case of a lasting overexploitation. *Science of the Total Environment* 906, 167723. <https://doi.org/10.1016/j.scitotenv.2023.167723>.
- Tumolo, M., Ancona, V., Paola, D., Losacco, D., Campanale, C., Massarelli, C., Uricchio, V.F., 2020. Chromium pollution in European water, sources, health risk, and remediation strategies: An overview. *International Journal of Environmental Research and Public Health* 17(15), 5438. <https://doi.org/10.3390/ijerph17155438>.
- United States Environmental Protection Agency, 1980. *Water Quality Criteria*.
- Wada, Y., Van Beek, L.P., Van Kempen, C.M., Reckman, J.W., Vasak, S., Bierkens, M.F., 2010. Global depletion of groundwater resources. *Geophysical Research Letters* 37(20). <https://doi.org/10.1029/2010GL044571>.
- WHO, 2021. *Silver in Drinking Water: Background Document for Development of WHO Guidelines for Drinking-water Quality (No. WHO/HEP/ECH/WSH/2021.7)*. World Health Organization.
- Zhang, B., Zhao, D., Zhou, P., Qu, S., Liao, F., Wang, G., 2020. Hydrochemical characteristics of groundwater and dominant water-rock interactions in the Delingha Area, Qaidam Basin, Northwest China. *Water* 12(3), 836. <https://doi.org/10.3390/w12030836>.